



Preparation and evaluation of injectable microsphere formulation for longer sustained release of donepezil

Yun Bae Ji^a, Soyeon Lee^a, Hyeon Jin Ju^a, Hee Eun Kim^a, Jung Hyun Noh^a, Sangdun Choi^a, Kinam Park^b, Hai Bang Lee^c, Moon Suk Kim^{a,c,*}

^a Department of Molecular Science and Technology, Ajou University, Suwon 443-749, Republic of Korea

^b Departments of Biomedical Engineering and Pharmaceutics, Purdue University, 206 S. Intramural Drive, West Lafayette, Indiana 47907-1791, United States of America

^c Research Institute, Medipolymers, Woncheon Dong 332-2, Suwon 16522, Republic of Korea



ARTICLE INFO

Keywords:
Microsphere
Donepezil
Injectability
Long-lasting release
Biodegradation
Inflammatory response

ABSTRACT

In this study, donepezil-loaded PLGA and PLA microspheres (Dp-PLGA-M/Dp-PLA-M) and Dp-PLA-M wrapped in a polyethylene glycol-*b*-polycaprolactone (PC) hydrogel (Dp-PLA-M/PC) were prepared to reduce the dosing frequency of injections to treat Alzheimer's disease patients. Dp-PLGA-M and Dp-PLA-M with a uniform particle size distribution were repeatedly fabricated in nearly quantitative yield and with high encapsulated Dp yields using an ultrasonic atomizer. The injectability and *in vitro* and *in vivo* Dp release, biodegradation, and inflammatory response elicited by the Dp-PLGA-M, Dp-PLA-M, and Dp-PLA-M/PC formulations were then compared. All injectable formulations showed good injectability with ease of injection, even flow, and no clogging using a syringe needle under 21-G. The injections required a force of <1 N. According to the biodegradation rate of micro-CT, GPC and NMR analyses, the biodegradation of Dp-PLA-M was slower than that of Dp-PLGA-M, and the biodegradation rate of Dp-PLA-M/PC was also slower. In the Dp release experiment, Dp-PLA-M sustained Dp for longer compared with Dp-PLGA-M. Dp-PLA-M/PC exhibited a longer sustained release pattern of two months. *In vivo* bioavailability of Dp-PLA-M/PC was almost 1.4 times higher than that of Dp-PLA-M and 1.9 times higher than that of Dp-PLGA-M. The variations in the Dp release patterns of Dp-PLGA-M and Dp-PLA-M were explained by differences in the degradation rates of PLGA and PLA. The sustained release of Dp by Dp-PLA-M/PC was attributed to the fact that the PC hydrogel served as a wrapping matrix for Dp-PLA-M, which could slow down the biodegradation of PLA-M, thus delaying the release of Dp from Dp-PLA-M. Dp-PLGA-M induced a higher inflammatory response compared to Dp-PLA-M/PC, suggesting that the rapid degradation of PLGA triggered a strong inflammatory response. In conclusion, Dp-PLA-M/PC is a promising injectable Dp formulation that could be used to reduce the dosing frequency of Dp injections.

1. Introduction

Alzheimer's disease (AD) is a progressive neurologic disorder that leads to slow and progressive memory loss, which sometimes results in language and behavioral issues that can interfere with daily life [1]. Donepezil (Dp), a specific and reversible cholinesterase inhibitor can effectively prevent and delay cognitive decline in patients with mild to moderate AD disease [2,3]. Until recently, Dp was only commercially available as orally administered tablets and capsules approved by the FDA. However, this medication is now available as a patch (*i.e.*, transdermal administration). AD patients must take tablets or capsules once a day or exchange the patch once every 2–3 days [4]. However, elderly AD

patients generally have difficulty swallowing pills or tablets, and patches are easily peeled off from their skin. In turn, this often results in poor treatment compliance in AD patients, leading to AD treatment discontinuation.

A slow-release Dp injection would provide a promising means to treat AD patients and improve patient compliance [5–7]. Some polymer-based drug delivery systems have been used for the development of rate control systems for drug release [8–10]. Poly(D,L-lactide-co-glycolide) (PLGA) microspheres are a promising vehicle for Dp delivery not only because they are FDA-approved but also because their small size allows for easy administration through intramuscular injection [11,12]. PLGA microspheres are widely used in injectable slow-release formulations of

* Corresponding author at: Department of Molecular Science and Technology, Ajou University, Suwon 443-749, Republic of Korea.

E-mail address: moonskim@ajou.ac.kr (M.S. Kim).

various drugs. The lactide/glycolide ratio, molecular weight and distribution, PLGA end group, and other factors are critical for the accurate control of the lag phase of drug release from microspheres [13].

Some studies have recently sought to prolong Dp release using Dp-loaded PLGA microspheres (Dp-PLGA-M) and improve patient compliance [14–17]. These studies demonstrated that Dp could be slowly released from Dp-PLGA-M for approximately one month, resulting in a prolonged and steady Dp release.

Furthermore, to fulfill future clinical demands for patient compliance, novel Dp-PLGA-M formulations could be developed to increase the Dp release period to more than one month. Alternatively, using other types of microspheres with longer release periods could further reduce injection frequency.

Therefore, one of the main objectives of this study was to develop a microsphere formulation that would enable the release of Dp for a period longer than one month. Dp can be released from microspheres in two main ways: (1) degradation/erosion of microspheres and (2) instantaneous diffusion of Dp from surface layer or inside of microspheres. To achieve this objective, our first aim was to control the release of Dp by modulating the degradation/erosion of microspheres, whereas our second aim was to delay the Dp released from the surface layer or inside of the microspheres.

Poly(D,L-lactide) (PLA) was selected to control the degradation/erosion of microspheres because this material is known to degrade relatively slowly compared with PLGA [18–22]. Therefore, PLA was incorporated into the microsphere formulation to control diffusion during the lag phase of Dp release. To the best of our knowledge, very few studies have described the use of Dp-loaded PLA microspheres (Dp-PLA-M) for the sustained release of Dp over a period longer than one month compared with Dp-PLGA-M.

In the process of Dp release from microspheres, the initial burst may occur because some amount of Dp tends to accumulate at or near the surface of the microspheres, thus inducing a rapid diffusion of Dp from the surface layer of the microspheres during the initial period. Therefore, several approaches to prevent the initial burst have focused on efficient encapsulation of the Dp inside PLGA-M rather than on the surface layer. However, complete elimination of the initial burst was often difficult or even impossible to achieve [23–26].

Recently, we reported an *in situ*-forming hydrogel [poly(ethylene

glycol-*b*-polycaprolactone (PC)] that can spontaneously form in response to body temperature, and the formed hydrogel can act as a drug depot [27–30].

To delay the Dp release from the microspheres, PC hydrogels were wrapped with Dp-PLA-M (Dp-PLA-M/PC) to achieve the second aim of this work. In this way, the Dp released from the surface layer or inside of the Dp-PLA-M could temporarily remain inside the PC hydrogel of Dp-PLA-M/PC. After the initial time, the Dp released from the Dp-PLA-M passed through the PC hydrogel and then moved to the subcutaneous layer at a delayed time, resulting in Dp release by lagging behavior. This delaying process can effectively control the diffusion of Dp release from the surface layer of or inside the Dp-PLA-M.

Here, we hypothesized that injectable Dp-PLA-M and Dp-PLA-M/PC formulations can create a Dp depot at the injected site, thus maintaining a therapeutic Dp concentration for longer than one month (Fig. 1). To the best of our knowledge, very few studies have characterized the slow-releasing properties of Dp-PLA-M and Dp-PLA-M/PC. Therefore, the present study sought to determine (1) whether Dp-PLA-M and Dp-PLGA-M can be reproducibly prepared in a simple and scalable way and with high Dp encapsulation efficiency and (2) verify if the Dp concentrations released from Dp-PLA-M and Dp-PLA-M/PC depots persist for an extended period in the injected site compared with Dp-PLGA-M. Therefore, the findings of this study would provide a theoretical and methodological basis for the development of an injectable slow-release Dp formulation to decrease Dp injection frequency and increase patient compliance.

2. Materials and methods

2.1. Materials

Donepezil (Dp; free base foam) was purchased from BOC Science (Shirley, NY, USA). Poly (D,L-lactide) (PLA; RESOMER R 203H, MW = 18,000–24,000) and poly (D,L-lactide-co-glycolide) (PLGA; RESOMER RG 503H, lactide/glycolide = 50/50, MW = 24,000–38,000) was purchased from EVONIK (Essen, Germany). Methoxy poly(ethylene glycol) (MPEG) (number-average molecular weight = 750), 1.0 M solution of HCl dissolved in ethyl ether, polyvinyl alcohol (PVA; 87%–89% hydrolyzed, MW = 85,000–124,000), fluorescein, ethyl acetate (EA), toluene,

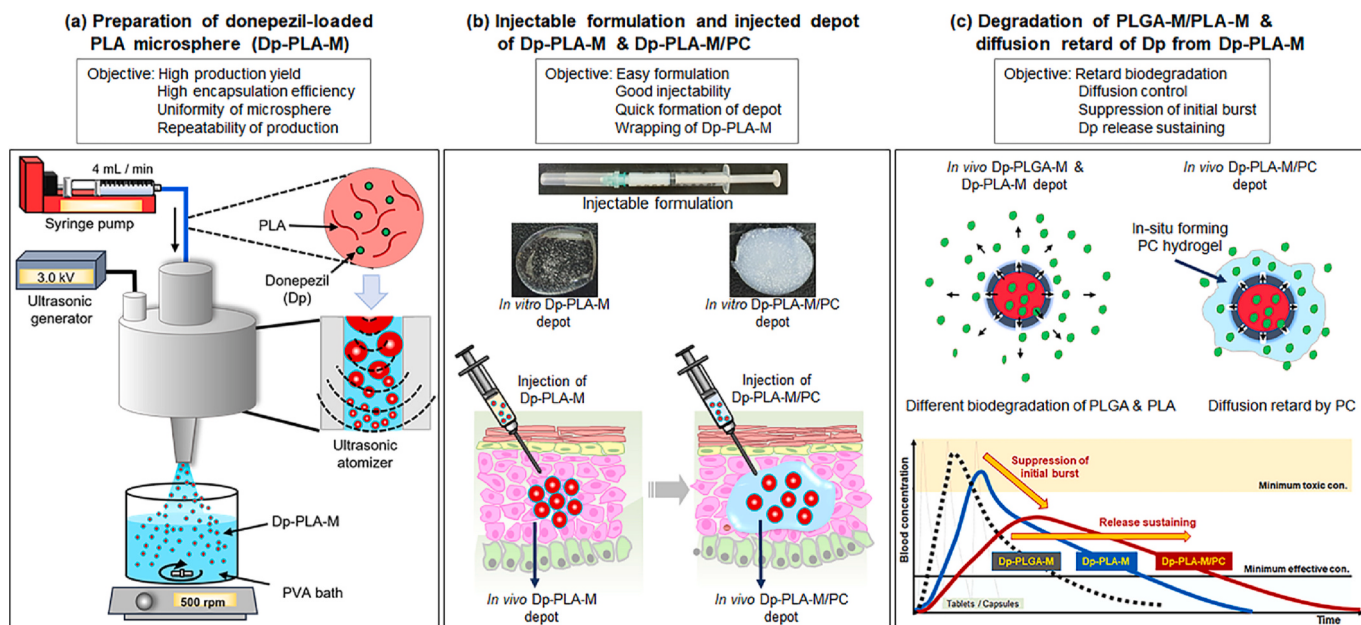


Fig. 1. Schematic representation of the preparation of (a) Dp-PLGA-M and Dp-PLA-M, (b) injectable formulation and depot formation, and (c) depot degradation and long-lasting Dp release from the depot.

n-hexane, ethyl ether, triethanolamine (TEA), phosphoric acid, mannitol, sodium carboxymethyl cellulose (Na-CMC) and Tween 80 were purchased from Sigma Aldrich (St. Louis, MO, USA). ϵ -Caprolactone (CL, TCI, Tokyo, Japan) was sequentially distilled from CaH_2 under nitrogen before use. Chloroform-D and acetone-D were purchased from Cambridge Isotope Laboratories, Inc. (MA, USA). Dulbecco's phosphate-buffered saline (DPBS) was purchased from Gibco (NY, USA). Dichloromethane (MC) was sequentially distilled from CaH_2 under nitrogen before use. Pure HPLC-grade acetonitrile (ACN), methanol (MeOH), ethanol, and tetrahydrofuran (THF) were obtained from different companies and used without further refinement.

2.2. Preparation of Dp-PLGA-M and Dp-PLA-M

Dp-PLGA-M and Dp-PLA-M were prepared using an ultrasonic atomizer (Sono-Tek Crop, Milton, NY, USA). Here, the weight ratios of PLA (or PLGA) and Dp were adjusted to 70:30, 65:35, and 60:40. To prepare the 65:35 ratio mixture, PLA (195 mg) and Dp (105 mg) were dissolved at 3 wt% in ethyl acetate and then evenly dissolved by vortexing. The PLA/Dp solution was loaded into a glass syringe (14.67 mm diameter). 250 mL of PVA solution (0.5% w/v PVA) was prepared in a beaker. The PVA solution was rotated at 500 rpm, and the distance between the atomizer head and the PVA solution was adjusted to 1 cm. Dp-PLA-M was produced by atomizing PLA/Dp solutions (to direction of PVA solution) at flow rates of 4 mL/min and a vibration frequency of 3 W/60 kHz. After atomizing, the resulting Dp-PLA-M was gently stirred for 2 h until it solidified. Then, the Dp-PLA-M solution was placed in a conical tube and washed five times with DW using a centrifuge (1500 rpm, 1 min, 4 °C). The resulting Dp-PLA-M was then filtered and once again washed five times with DW. The Dp-PLA-M was frozen at –74 °C, followed by freeze-drying for over 3 days. Fluorescein-loaded PLA microspheres (FI-PLA-M) were prepared from PLA (180 mg) and FI (120 mg) by the same procedures as described in the previous paragraph.

Dp-PLA-M at two different high doses of PLA (900 or 1800 mg) and Dp (600 or 1200 mg) was fabricated in the same way as PLA (195 mg) and Dp (105 mg). **Tables S1** and **S2** summarize the characteristic analysis of Dp-PLGA-M and Dp-PLA-M.

2.3. Synthesis of methoxy poly(ethylene glycol)-block-polycaprolactone diblock copolymers (PC)

PC with a molecular weight of 2420 g/mol per polycaprolactone segment was prepared at a 95% yield and polydispersity of 1.17 via gel permeation chromatography (GPC) as previously reported [27–30].

2.4. Preparation of injectable formulation (Dp-PLGA-M, Dp-PLA-M, and Dp-PLA-M/PC)

The injection solution was prepared by dissolving mannitol (5%), Na-CMC (2%), and Tween 80 (0.1%) in DPBS. PC (75 mg) was mixed in 0.3 mL of DPBS to reach a 20 wt% concentration and solubilized at 70 °C by vortexing. The PC solution was stabilized at 4 °C for 2 days. Next, Dp-PLGA-M (51.4 mg) or Dp-PLA-M (48.9 mg) was loaded into 300 μL of the injection solution or PC solution to obtain Dp-PLGA-M/PC and Dp-PLA-M/PC. The Dp concentration per injectable formulation was 16.8 mg.

2.5. Encapsulation efficiency and in vitro release of Dp-PLGA-M, Dp-PLA-M, and Dp-PLA-M/PC

The Dp encapsulation efficiency and release rates of Dp-PLGA-M, Dp-PLA-M, and Dp-PLA-M/PC were determined by high-performance liquid chromatography (HPLC; Agilent Technologies 1200 series; Agilent Technologies, California, USA) using a Shiseido UG120 C₁₈ packing column (250 × 4.6 mm, 5 μm ; Sigma-Aldrich, St. Louis, MO, USA) at a flow rate of 1.2 mL/min, with absorbance detection at 268 nm and at a 40 °C column temperature.

First, buffer A was prepared by adding 50 mL of THF and 14 mL of TEA to 1000 mL of DW, after which phosphoric acid was added to adjust the pH of the solution to 2.0. The HPLC mobile phase was prepared by mixing buffer A and methanol at a 3:2 ratio. Then, equal volumes (1:1 ratio) of buffer A and ACN (buffer B) were mixed and used to measure the Dp encapsulation rate in Dp-PLGA-M and Dp-PLA-M and to determine the Dp release rates from Dp-PLGA-M, Dp-PLA-M, and Dp-PLA-M/PC.

To determine the Dp encapsulation rate, 10 mg of Dp-PLGA-M and Dp-PLA-M were solubilized in 4 mL of buffer B, vortexed and sonicated for 10 min at 25 °C, and passed through a PVDF filter (0.45 μm). Three independent measurement experiments were performed for Dp-PLGA-M and Dp-PLA-M.

The Dp loading efficiency was defined as follows: LE (%) = [(encapsulated Dp weight) / (obtained microspheres weight)] × 100. The encapsulation efficiency (E) was defined as follows: E = [(amount of encapsulated Dp) / (total amount of Dp added)] × 100.

2.6. Characterization of Dp-PLGA-M, Dp-PLA-M, and Dp-PLA-M/PC

The optical images of Dp-PLGA-M and Dp-PLA-M were obtained using an Axio Imager A1 microscope (Carl Zeiss Microimaging GmbH, Göttingen, Germany) coupled with the Axiovision Rel. 4.8 software (Carl Zeiss) and a Camscope system (Somotech, Seoul, Korea) with a SuperCast U6T 2HD (Skydigital, Goyang, Korea). The surface morphology of Dp-PLGA-M and Dp-PLA-M were observed using a field emission scanning electron microscope (FE-SEM; JSM-7900F; JEOL, Tokyo, Japan). Dp-PLGA-M and Dp-PLA-M were thinly coated using a plasma sputtering apparatus (Ted Pella, Cressington 108 Auto, Redding, CA, USA) under argon and then captured at a 500 \times magnification.

The particle size and particle size distribution of Dp-PLGA-M and Dp-PLA-M were measured via dynamic light scattering analysis (DLS; ELSZ-1000; Otsuka Eletronics, Osaka, Japan). Ten milligrams of Dp-PLGA-M or Dp-PLA-M were evenly dispersed with 1 mL of deionized water (DW). The particle size and particle size distribution were calculated using ELS-Z version 3.8 (Otsuka, Japan). Three independent measurements were performed for each Dp-PLGA-M or Dp-PLA-M. All data are presented as means ± standard deviation (SD). The span value of Dp-PLA-M or Dp-PLGA-M was defined as follows: [(90% at particle size – 10% at particle size) / (50% at particle size)] × 100 [14].

To assess the stability of the Dp-PLGA-M or Dp-PLA-M, all microspheres were incubated at 4, 37, and 60 °C for 4 weeks. At 1, 2, 3 and 4 weeks, 10 mg of the Dp-PLGA-M or Dp-PLA-M were dissolved in DW at a 1 wt% concentration and the particle sizes were measured three times by dynamic light scattering described in the previous section. All results are presented as means ± standard deviation.

The mechanical properties including Young's (elastic) modulus and hardness of Dp-PLGA-M, Dp-PLA-M, and Dp-PLA-M/PC were measured using a nano-indenter (NanoTest NTX; Micro Materials, Wrexham, UK) with a three-sided pyramidal Berkovich tip.

2.7. Rheological characterization of Dp-PLGA-M, Dp-PLA-M, and Dp-PLA-M/PC

The rheological properties of the injectable formulations of Dp-PLGA-M, Dp-PLA-M, and Dp-PLA-M/PC prepared in the previous section were measured using a modular compact rheometer (MCR 102, Anton Paar, Austria) with a Peltier temperature-controlled bottom platen. The parallel plate diameter was 25 mm. All measurements were conducted with a gap length of 0.3 mm at a frequency of 1 Hz and 1% strain from 10 to 60 °C. The storage modulus (G') and loss modulus (G''), viscosity (cP) and the phase angle ($\tan \delta$) were calculated using the instrument's software (Rheoplus/32, version V3.21, Anton Paar, Austria). Each sample was measured three times.

2.8. Evaluation of the injection force of Dp-PLGA-M, Dp-PLA-M, and Dp-PLA-M/PC

The formulation of injection solution alone [mannitol (5%), Na-CMC (2%), and Tween 80 (0.1%) in DPBS], PC solution alone [100 mg of PC solubilized in 0.4 mL of DPBS], Dp-PLGA-M [68.5 mg of Dp-PLGA-M solubilized in 400 μ L of injection solution], Dp-PLA-M [65.2 mg of Dp-PLA-M solubilized in 400 μ L of injection solution], Dp-PLGA-M/PC [68.5 mg of Dp-PLGA-M solubilized in 400 μ L of PC solution], and Dp-PLA-M/PC [65.2 mg of Dp-PLA-M solubilized in 400 μ L of PC solution] was prepared. The Dp concentration per injectable formulation was 16.8 mg. Next, 400 μ L of the injection solution alone, PC solution alone, Dp-PLGA-M, Dp-PLA-M, and Dp-PLA-M/PC were separately loaded into single-barrel syringes. The inner diameters of the syringe needle gauge were 21-G (0.495 mm inner diameter), 23-G (0.318 mm inner diameter), and 26-G (0.241 mm inner diameter).

Injection force was determined using a universal testing machine (H5KT, Tinius-Olsen, Horsham, PA, USA). The plunger end of the syringe was placed in contact with a 500 N loading cell. The measurement was performed at 1 mm/s, which is the typical speed when injecting a patient. The injection force of each formulation was measured in compressive strength mode using compression mode software (Tinius Olsen, Rock Hill, SC, USA). The injection force of each formulation was measured three times. Each formulation was plotted as force-injection volumes. The F_{\max} and DGF (dynamic glide force) values of 300 μ L of each formulation were defined as the value in the range maintaining linearity and the highest value in the force-displacement plots, respectively.

2.9. In vitro drug release of each injectable formulation

The injectable formulations of Dp-PLGA-M, Dp-PLA-M, and Dp-PLA-M/PC (all containing 16.8 mg of Dp) prepared in the previous section were loaded into a tube with a dialysis membrane at the bottom (Slide-A-Lyzer MINI Dialysis units, 2.0 K MWCO; Thermo Fisher Scientific, Waltham, Massachusetts, USA). Each tube with each injectable formulation was individually placed in a 50 mL conical tube containing 45 mL of DPBS and then incubated at 37 °C and 100 rpm. For each experiment, 25 mL of DPBS solution was extracted from the conical tube at predetermined time intervals and 25 mL of fresh DPBS incubated at 37 °C was immediately added to the vials to restore the volume. The amount of Dp released from Dp-PLGA-M, Dp-PLA-M, and Dp-PLA-M/PC was determined by HPLC, as described in a previous subsection, and calculated through a comparison with standard calibration curves constructed using known concentrations of Dp. Three independent release experiments were conducted for each formulation and the results were presented as mean \pm standard deviation.

2.10. Animal experiments

The protocol for the animal experiments was approved by the Institutional Animal Care and Use Committee (Approval No. 2021–0009) of the Ajou University School of Medicine. All experiments were performed using SD rats (300 g, male, 6 weeks) in accordance with the guidelines for the care and use of animals for experimental and scientific purposes.

Injectable formulations of Dp-PLGA-M, Dp-PLA-M, and Dp-PLA-M/PC (Dp 16.8 mg) prepared in the previous section were sterilized by ultraviolet irradiation (254 nm) for 2 h. During ultraviolet irradiation, the injectable formulations were rotated every 30 min to ensure uniform sterilization.

SD rats were anesthetized with 1:1 Zoletil-Rompun solution (37.5 mg/kg). Each injectable formulation was loaded into a syringe with a 21-gauge needle. Each injectable formulation (300 μ L) in the syringe was injected subcutaneously into SD rats and the subcutaneous generation of depots (Dp-PLGA-M, Dp-PLA-M, and Dp-PLA-M/PC) was

confirmed. The injected SD rats were sterilized with povidone and provided with sufficient water and food throughout the experimental period. At predetermined time intervals, the injected SD rats were euthanized using CO₂ in accordance with animal guidelines and then each depot was removed.

2.11. Characterization of in vivo depots formed from Dp-PLGA-M, Dp-PLA-M, and Dp-PLA-M/PC

The depots (Dp-PLGA-M, Dp-PLA-M, and Dp-PLA-M/PC) were allowed to develop and were then subjected to biopsy at different time points over eight weeks. At each of the post-implantation points (1, 3, 6, and 8 weeks), the rats were sacrificed, and the depots were individually dissected and removed from the subcutaneous dorsum to conduct optical morphology, micro-CT, SEM, NMR, and GPC analyses.

Optical images of the removed depot were obtained using an optical camera and a ruler. The depot volume was calculated based on the optical depot images using the following formula: $0.52 \times \text{width} \times \text{length} \times \text{height}$. The morphology of the removed depots was also observed using a Camscope system (Sometech, Seoul, Korea) and an optical microscope (Nikon, Labophot-2, Japan) using a lens magnification of 100 \times and 300 \times .

The removed depots were further analyzed via microcomputed tomography (micro-CT; Skyscan 1076; Skyscan, Konitch, Belgium). Micro-CT was carried out with a high-resolution Explore Locus scanner (GE Healthcare, Ontario, Canada) at an 18.22 μ m pixel resolution, a 340 ms exposure time, a 59 kV energy source, and a 153 μ A current. Approximately 180 projections were acquired over a rotation range of 180°, with a rotation step of 4°. The full length of each depot was scanned and consisted of 850 slices on average. Three-dimensional virtual models for the estimation of depot volume were created and visualized using the micro view image processing MIMICS 16.0 software (Materialise's Interactive Medical Image Control System; Leuven, Belgium).

A field emission scanning electron microscope (FE-SEM; JSM-7900F; JEOL, Tokyo, Japan) was used to examine the morphology of the *in vivo* depots. The removed depots were immediately immersed in a liquid nitrogen bath to minimize structural changes in the depots, then freeze-dried for 5 days at -75 °C and finally cut in the cross-sectional direction in a liquid nitrogen environment to minimize alteration of the depots. The prepared depots were then coated with a thin layer of gold using a plasma-sputtering apparatus (Ted Pella, Cressington 108 Auto, Redding, CA, USA) in an argon atmosphere and examined by SEM (PC-SEM; JEOL, Tokyo, Japan). The depots measured by SEM were recovered and cross-sectional images were obtained using Camscope.

The removed depots were placed in a test tube to which chloroform (5 mL) was added and pulverized using a homogenizer at 16,000 rpm and 25 °C for 10 min to dissolve the polymer portion of the depot. Then, the mixture was sonicated at 25 °C for 30 min and centrifuged at 4000 rpm and 4 °C for 10 min. The supernatant from the obtained suspension was filtered using a PTFE filter (0.45 μ m). The filtered solution was rotary evaporated and dried under reduced pressure to completely remove all traces of chloroform. The obtained sample was analyzed by NMR and gel permeation chromatography (GPC) to examine biodegradation. Some of the obtained mixtures were precipitated in *n*-hexane and ether (4:1), filtered with filter paper, separated to obtain soluble and insoluble fractions, and dried at 4 °C for 2 days in a vacuum oven. The dried soluble and insoluble parts were measured by GPC using a Futecs GPC 500 system coupled with a Shodex 201H RI detector (Futecs, Daejeon, Korea) and polystyrene gel columns (Shodex K-802, K-803, and K-804) in CHCl₃ at 40 °C as an eluent at a flow rate of 1 mL/min. Polystyrene standards were used for calibration and to determine the relative molecular weight and the distribution of the molecular weight. The degradation ratio was defined as follows: Degradation ratio (%) = [MW determined at the GPC peak at the predetermined time points] / MW determined at the GPC peak on week 0] \times 100. The obtained degradation ratios were plotted as a function of time to determine the

first-order rate constant. The *in vivo* half-life degradation was defined as the time required to degrade half of the initial molecular weight.

2.12. Dp release from *in vivo* depots formed from Dp-PLGA-M, Dp-PLA-M, and Dp-PLA-M/PC

The Dp-PLGA-M, Dp-PLA-M, and Dp-PLA-M/PC depots (Dp 16.8 mg) injected in the previous section were individually dissected and removed from the subcutaneous dorsum at 1, 2, 3, 4, 6, and 8 weeks. The tissue on the surface of the extracted depot was removed as thoroughly as possible using surgical scissors. The trimmed depots were then placed in a test tube to which ACN (8 mL) was added and homogenized using a homogenizer at 16,000 rpm and 25 °C for 10 min to dissolve the Dp drug portion of the depot. The mixture was then sonicated at 25 °C for 30 min and centrifuged at 2000 rpm and 4 °C for 10 min. The supernatant from the obtained suspension was then passed through a PTFE filter (0.45 µm). The filtered solution was rotary evaporated and dried under reduced pressure to completely remove all can traces. The obtained sample was analyzed by HPLC to examine the remaining Dp inside the depot at different time points. The remaining Dp inside the depots at different time points was calculated based on standard calibration curves constructed using known concentrations of Dp.

The ratio of the cumulative Dp released *in vivo* was defined as follows: cumulative ratio of Dp released *in vivo* (%) = [(Total amount of injected Dp (16.8 mg) on day 0 – Dp inside the depot extracted at the predetermined time points) / Total amount of injected Dp on day 0] × 100. Each release Dp experiment was individually performed for three rats and the results were presented as mean ± standard deviation.

2.13. Histological analysis of *in vivo* depots

The Dp-PLGA-M, Dp-PLA-M, and Dp-PLA-M/PC depots injected in the previous section of were individually removed from the subcutaneous dorsum at 1, 3, 6, and 8 weeks. The removed depots were immediately fixed with 10% formalin for two days. The paraffin wax-embedded specimens were sliced into 5-µm-thick sections along the longitudinal axis of the depot.

Deparaffinization and hydration were performed by immersing the slides (5 min per immersion) in xylene two times, 100% ethanol two times, 95% ethanol one time, and 70% ethanol one time. Afterward, the depot samples were treated with a hematoxylin solution (Sigma-Aldrich, St. Louis, MO, USA) for 3 min, washed with running water, and treated with eosin for 6 min, then once again washed with running water to obtain H&E-stained images. After drying the slide for 3 h at room temperature, the slides were mounted with a mounting solution (Muto Pure Chemicals; Tokyo, Japan).

To perform CD4 and CD68 (ED1) staining, the slides were deparaffinized and hydrated in the same way as with H&E staining. The slides were then immersed in 1× HIER T-EDTA buffer (pH 9.0) and incubated at 130 °C for 20 min prior to antigen recovery. After cooling at room temperature, the slides were washed in PBS and blocked at 25 °C for 60 min using PBS solution with 5% horse serum and 0.3% Triton X-100. The samples were then treated with CD4 antibodies (mouse anti rat CD4; Serotec, Oxford, UK) or CD68 antibodies (mouse anti rat CD68; Serotec, Oxford, UK) at a 1:500 dilution ratio in antibody diluent at 4 °C for 12 h. The slides were washed with PBS and PBST (0.05% Tween-80 in PBS), then treated with secondary antibodies (Alexa Fluor 594 goat anti-mouse IgG; Invitrogen, Waltham, MA, USA) at a 1:500 dilution ratio in antibody diluent at room temperature for 3 h. The samples were then washed with PBS and PBST and treated with a 1 µg/mL DAPI solution. After thoroughly washing the samples with DW, the slides were mounted using a mounting solution. The stained slides were then visualized using a slide scanner (ZEISS Axio Scan. Z1, Carl Zeiss Microscopy GmbH, Jena, Germany). The quantitative evaluation of the stained images was performed with $n = 3$ for each data point using the ImageJ program.

2.14. Statistical analyses

All data were obtained from three independent experiments and were presented as the mean ± standard deviation (SD). To evaluate significance, the results were subjected to one-way analysis of variance (ANOVA) coupled with Bonferroni's multiple-comparison correction using the SPSS 12.0 software (SPSS Inc., Chicago, IL, USA).

3. Results

3.1. Preparation and characterization of Dp-PLGA-M and Dp-PLA-M

In this study, the Dp-PLGA-M and Dp-PLA-M were fabricated using an ultrasonic atomizer (Fig. S1). To achieve this, the ultrasonic atomizer was loaded with a solution of PLGA or PLA and Dp in ethyl acetate. The atomization process resulted in the formation of emulsion microdroplets as they were sprayed through the nozzle tip. Afterward, the ethyl acetate from the emulsion microdroplets was evaporated and extracted in deionized water containing polyvinyl alcohol (PVA), resulting in the formation of Dp-PLGA-M and Dp-PLA-M. The resulting Dp-PLGA-M and Dp-PLA-M exhibited a 94% average yield, an average encapsulation efficiency of 93%, and a particle size of 61–67 µm (Fig. S1 and Table S1). FI-PLA-M was greenish due to the color of FI. FI-PLA-M had a size, surface, and shape similar to those of Dp-PLA-M.

The obtained Dp-PLA-M were stable at 4 °C and 37 °C for 4 weeks, but Dp-PLGA-M showed the stability only at 4 °C for 4 weeks (Fig. S2). Meanwhile aggregation of Dp-PLGA-M and Dp-PLA-M was observed at 60 °C even at 1 week due to the glass transition temperature of PLGA and PLA.

The obtained Dp-PLGA-M and Dp-PLA-M were generally uniform regardless of the Dp contents and the type of polymer used to fabricate them. Both the Dp-PLGA-M and Dp-PLA-M exhibited a spherical shape with a smooth surface. Additionally, the Dp-PLA-M were obtained with a nearly quantitative production yield and high encapsulation Dp yield after repeated manufacturing of large amounts (Table S2).

The span value is generally used as an indicator of particle size uniformity [11]. In this study, the span values of both Dp-PLGA-M and Dp-PLA-M were close to one, meaning that the fabricated microspheres were uniform.

Furthermore, previous studies have reported that microspheres should not exceed a size of ~100 µm for easy subcutaneous or intramuscular injection using 21–25-G needles [31,32]. Therefore, the subcutaneous injection of the manufactured Dp-PLGA-M and Dp-PLA-M is expected to be relatively painless.

Interestingly, the microspheres without Dp, which were fabricated several times, were smaller in the absence of Dp. This was likely because Dp interrupted the compact aggregation between the polymer chains, resulting in larger Dp-PLGA-M and Dp-PLA-M particles.

Finally, the uniformity and repeatability of the proposed Dp-PLGA-M and Dp-PLA-M fabrication method was verified, and the manufactured Dp-PLGA-M and Dp-PLA-M were used for subsequent *in vitro* and *in vivo* experiments.

3.2. Rheological characterization of Dp-PLGA-M and Dp-PLA-M

The hydrophobicity, T_g , and crystallinity of PLA, which contains methyl side groups, were generally different from those of PLGA [33,34]. Therefore, a nanoindentation measurement was performed to compare the mechanical properties of Dp-PLGA-M and Dp-PLA-M with a 35% Dp concentration, after which hardness values were calculated based on the obtained measurements (Fig. 2a-c).

When a force was applied to the surface of the Dp-PLGA-M and Dp-PLA-M using a Berkovich tip, Dp-PLA-M showed a higher value than Dp-PLGA-M, indicating that the surface of Dp-PLA-M was harder. The Young's modulus (*i.e.*, elastic modulus) value of Dp-PLA-M was approximately 1.5 times higher than that of Dp-PLGA-M. Similarly, the

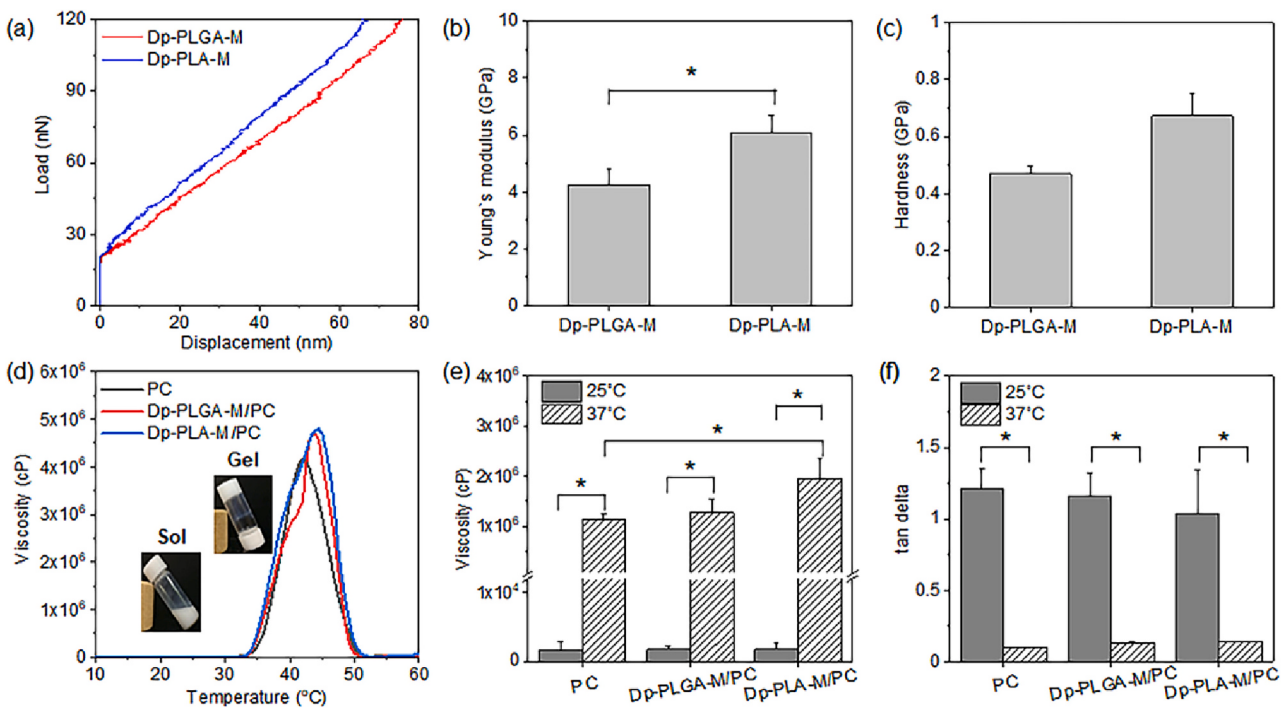


Fig. 2. (a-c) Nanoindentation tests of Dp-PLGA-M and Dp-PLA-M; (a) load-displacement curves, (b) Young's (elastic) modulus and (c) hardness of Dp-PLGA-M and Dp-PLA-M (* $p < 0.01$). (d-f) Rheological characterization of PC alone, Dp-PLGA-M/PC, and Dp-PLA-M/PC. (d) Viscosity-versus-temperature curves, (e) viscosity at 25 °C and 37 °C, and (f) results of the phase angle experiment (* $p < 0.01$).

hardness of Dp-PLA-M was approximately 1.5 times higher than that of Dp-PLGA-M, indicating that the Dp-PLA-M did not deform easily due to the resistance of PLA to the applied force.

Collectively, our findings indicated that the mechanical properties of Dp-PLGA-M and Dp-PLA-M can be adjusted by changing the matrix polymers (PLGA and PLA).

3.3. Preparation and characterization of injectable formulations

In this work, thermosensitive PC hydrogel was applied to reduce the initial burst of Dp from outermost surface of the microspheres because PC showed a sol-to-gel phase transition at body temperature [27–30]. Therefore, we mixed PC with Dp-PLGA-M and Dp-PLA-M to conduct a comparative rheological characterization.

The rheological characterization of PC alone, Dp-PLGA-M/PC, and Dp-PLA-M/PC was conducted as a function of temperature (Fig. 2d-f). PC alone, Dp-PLGA-M/PC, and Dp-PLA-M/PC showed a viscosity of 1, exhibiting a solution state at approximately 30 °C. However, their viscosity increased rapidly to 1.06×10^6 cP, 1.36×10^6 cP, and 1.70×10^6 cP at 37 °C (Fig. 2d-f). This confirmed that PC alone, Dp-PLGA-M/PC, and Dp-PLA-M/PC could form hydrogel depots at 37 °C (*i.e.*, body temperature) due to the thermosensitive behavior of PC.

The phase angles ($\tan \delta$) of PC alone, Dp-PLGA-M/PC, and Dp-PLA-M/PC calculated from G''/G' were respectively 1.21, 1.16, and 1.04 at 25 °C, thus demonstrating the elasticity of these materials. However, these values changed to 0.10, 0.13, and 0.14 (*i.e.*, substantially <1) at 37 °C, indicating that microsphere formulations with PC hydrogel (Dp-PLGA-M/PC, and Dp-PLA-M/PC) exhibited more hydrogel-like properties at body temperature than PC alone (Fig. 2f).

Furthermore, even though there was little difference between Dp-PLGA-M/PC and Dp-PLA-M/PC, the phase angle of Dp-PLA-M/PC was slightly lower than that of Dp-PLGA-M/PC, indicating that the Dp-PLA-M/PC formulation showed hydrogel-like properties at body temperature. Taken together, our findings indicated that Dp-PLA-M/PC were slightly stiffer and more hydrogel-like than Dp-PLGA-M/PC.

3.4. Injectability of Dp-PLGA-M, Dp-PLA-M, and Dp-PLA-M/PC formulations

First, we sought to verify whether all injection formulations were uniformly distributed in depots formed from suspension after the injection of all formulations. Examination of the injected depot demonstrated that the microspheres were uniformly spread in the suspension (Fig. 3a-b). Fluorescent or optical images of all injection formulations before and after injection showed a homogeneous distribution in fluorescence of FI-PLA-M or homogeneous sphere shape of PLA-M (Fig. S3). This indicated that all injection formulations were prepared in a facile manner and the PLA microspheres were uniformly dispersed inside injection solution or PC hydrogel.

Next, the effect of the injection formulations and the gauge sizes of the syringe needle on injectability was evaluated. Specifically, we evaluated whether the formulations could be easily injected without needle clogging by pushing the syringe plunger by hand. The extrusion for each formulation of injection solution alone, PC alone, Dp-PLGA-M, Dp-PLA-M, Dp-PLGA-M/PC, and Dp-PLA-M/PC in a single-barrel syringe with 21-G, 23-G, and 26-G needles was individually evaluated to assess the injectability of the injectable formulations.

Extrusion proceeded without clogging a 21-G needle until all injectable formulations were consumed. However, extrusion of Dp-PLGA-M, Dp-PLA-M, Dp-PLGA-M/PC, and Dp-PLA-M/PC needed additional force or did not come out from 23-G and 26-G needles due to clogging of the injectable formulations. These findings indicated that syringe needles under 21-G were suitable for injection of the formulations.

Additionally, the injectability of all injection formulations was quantified using a universal testing machine (Figs. 3c-e). The loading force (injecting force) and injection volume of all injection formulations were plotted based on a constant injection rate (1 mm/s) according to the type of injection formulations and the gauge sizes of the syringe needle.

When the injection force of all injectable formulations was measured using a 21-G needle, the injection force was initially high (F_{max}), after

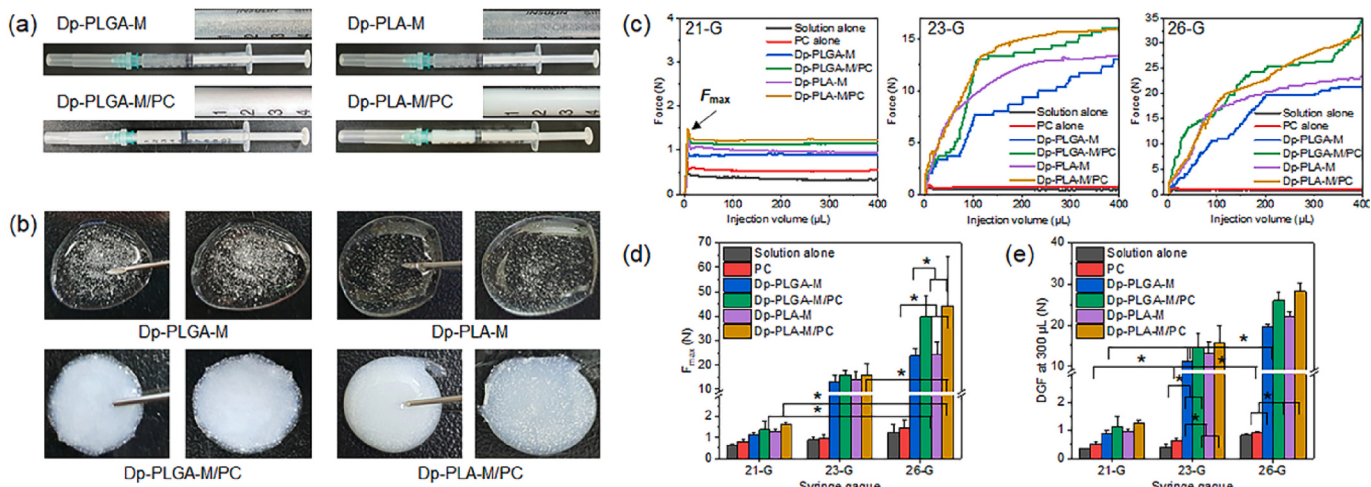


Fig. 3. Optical images of (a) injectable formulations of Dp-PLGA-M, Dp-PLA-M, Dp-PLGA-M/PC, and Dp-PLA-M/PC loaded into a syringe and (b) Dp-PLGA-M, Dp-PLA-M, Dp-PLGA-M/PC, and Dp-PLA-M/PC depot formed after injection of each formulation. Injectability tests of (c) injection solution alone, PC alone, Dp-PLGA-M, Dp-PLA-M, Dp-PLGA-M/PC, and Dp-PLA-M/PC formulation loaded into a syringe. (d) Loading F_{max} and dynamic glide force (DGF) that must be applied to the syringe plunger to expel 300 \$\mu\$L of each injectable formulation from 21-G, 23-G, and 26-G needles as a function of time at a loading force speed of 1 mm/s (* $p < 0.01$).

which a constant force was maintained until all injectable formulations were consumed. The initial injection force (F_{max}) of the injection solution alone and PC alone showed low a F_{max} value of 1 N or less. In contrast, the F_{max} of Dp-PLGA-M, Dp-PLA-M, Dp-PLGA-M/PC, and Dp-PLA-M/PC (all containing 16.8 mg of Dp) increased to 1.1–1.6 N (Fig. S4). After the F_{max} , all injection formulations exhibited a constant force and slightly lower values than F_{max} , meaning that all injection formulations could pass through the needle at a constant force.

Next, when the injection force of the injection solution alone and PC alone was measured using a 23-G needle, the injections could still be administered with no problem even though the F_{max} increased up to 1 N. However, the F_{max} of Dp-PLGA-M, Dp-PLA-M, Dp-PLGA-M/PC, and Dp-PLA-M/PC increased to approximately 13–16 N. These values were due to the narrow inner diameter of the syringe needle, which increased the resistance of the solutions passing through the needles. In the 26-G needle, the F_{max} of the injection solution alone and PC alone slightly increased to approximately 1.36–1.5 N but this value was still considered low. However, the F_{max} of Dp-PLGA-M, Dp-PLA-M, Dp-PLGA-M/PC, and Dp-PLA-M/PC increased to approximately 24–44 N.

Taken together, our findings indicated that 21-G needles were suitable for the administration of all injection formulations tested herein, and therefore these needles were used for all subsequent *in vitro* and *in vivo* experiments.

3.5. *In vitro* drug release of Dp-PLGA-M, Dp-PLA-M, and Dp-PLA-M/PC depot

To examine the sustained release of Dp *in vitro*, we compared the Dp release between Dp-PLGA-M and Dp-PLA-M prepared in different carriers, and between Dp-PLA-M and Dp-PLA-M/PC with and without PC hydrogel wrapping.

The *in vitro* patterns of Dp release from Dp-PLGA-M, Dp-PLA-M, and Dp-PLA-M/PC were examined at 37 °C for 84 days (Fig. 4). The cumulative amount of Dp released from the Dp-PLGA-M and Dp-PLA-M was 16% and 7% on day 4, followed by 32% and 12% on day 7. The cumulative Dp release amount from Dp-PLGA-M showed a linear pattern up to 63% for 14 days but reached almost 99% at 35 days with a slight decrease in the release slope after 14 days.

Moreover, Dp-PLA-M showed little retardation of the Dp release throughout the first 7 days, after which it exhibited a Dp release slope and a pattern similar to that of Dp-PLGA-M at 35 days. Due to the initial retardation of the Dp release, the Dp release reached 96% at 56 days. This was likely because PLA is more hydrophobic than PLGA. Additionally, Dp-PLA-M is a harder material than Dp-PLGA-M, as described above.

Dp-PLA-M resulted in a longer and more sustained Dp release than Dp-PLGA-M for the entire release period as the first aim of this work. The difference in Dp release between Dp-PLGA-M and Dp-PLA-M was

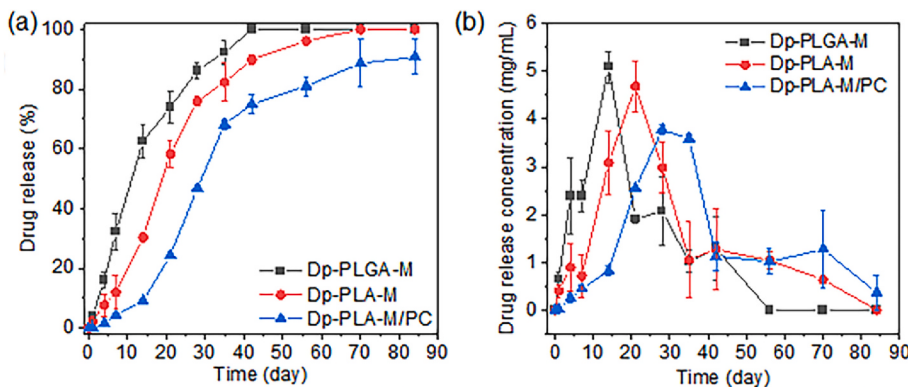


Fig. 4. *In vitro* drug release of the Dp-PLGA-M, Dp-PLA-M, and Dp-PLA-M/PC formulations. (a) Accumulated *in vitro* release behavior of Dp from Dp-PLGA-M, Dp-PLA-M, and Dp-PLA-M/PC depots for 84 days and (b) Dp concentration released from each depot at each time point.

modulated through the degradation of PLGA and PLA.

Therefore, the PC hydrogel was only wrapped with Dp-PLA-M to maintain the Dp release for a period longer than two months. Upon comparing the Dp release from Dp-PLA-M and Dp-PLA-M/PC, Dp-PLA-M/PC exhibited a more long-lasting Dp release pattern than that of Dp-PLA-M. This long-lasting Dp release pattern likely occurred because the Dp released in the early period remained in the PC hydrogels that acted as wrapping materials. Afterward, the sustained release with a lower burst effect in the early period could be attributed to a greater retardation of Dp for the entire release period. This result indicated that Dp-PLA-M acted as a depot of Dp at first, after which the PC hydrogel served as a depot because it was wrapped around the microspheres.

Collectively, this long-lasting Dp release of Dp-PLA-M/PC was attributed to a suppression of Dp release during the early period, resulting in a longer and more sustained Dp release for the entire release period.

3.6. In vivo drug release of the Dp-PLGA-M, Dp-PLA-M, and Dp-PLA-M/PC depots

To compare the *in vivo* Dp release behavior, the Dp-PLGA-M, Dp-PLA-M, and Dp-PLA-M/PC formulations were prepared and then intramuscularly injected into Sprague-Dawley (SD) rats (Fig. 5a). All formulations immediately formed a Dp depot at the injected sites. No adverse symptoms (self-harm, vomiting, weight loss) were observed in the SD rats during the experimental period. The Dp depots formed in the live SD rats were removed at predetermined times. Thin fibrous capsules containing fibroblasts and vascular vessels formed around the surfaces of the formed Dp depots.

Next, the released amount of Dp was calculated by comparing the amount of Dp remaining in the extracted Dp depot at each predetermined time with the amount of Dp initially injected, and the results were then plotted (Fig. 5b). On day 1, the released Dp amounts from Dp-PLGA-M and Dp-PLA-M were approximately 23%–24% due to a slight

initial burst regardless of the microsphere material (PLGA or PLA). Then, Dp-PLGA-M showed 63% at 4 days, 84% at 1 week, 91% at 2 weeks, and 97% at 4 weeks. Dp-PLA-M showed 38% at 4 days, 46% at 1 week, 64% at 2 weeks, 81% at 3 weeks, and 97% at 4 weeks. Dp release from Dp-PLA-M tended to be more gradual and sustained than that of Dp-PLGA-M. This result indicated that Dp release was affected by the properties of the polymer matrix of the microspheres, which was consistent with the results of the *in vitro* experiments.

In the case of Dp-PLA-M/PC, approximately 10% of Dp was released on day 1. This result indicated that the initial release of Dp was delayed by the PC layer wrapping the Dp-PLA-M. Therefore, Dp release was two times lower than that of Dp-PLGA-M and Dp-PLA-M. After day 1, the Dp released from Dp-PLA-M exhibited continuously delayed profiles for 56 days.

The Dp concentration released per release time was quantified to perform pharmacokinetic analysis of Dp release data over time (Fig. 5c). In the case of PLGA-M, the release rate of Dp reached its maximum at 4 days and most of the Dp was released in 21 days. After 21 days, the remaining Dp was completely released. PLGA-M exhibited a Dp burst and then biphasic Dp release profiles *in vivo*.

Dp-PLA-M showed a lower Dp release rate from day 1 (at faster time) to 7 *in vivo* due to a slight suppression of the initial Dp burst compared to Dp-PLGA-M. Afterward, the Dp released amount increased and a relatively constant amount of Dp was steadily released for 28 days. After 28 days, the remaining Dp was completely released.

Dp-PLA-M/PC showed a similar release pattern to that of Dp-PLA-M. In contrast, Dp-PLA-M/PC showed a lower Dp release amount than Dp-PLA-M on day 1, and Dp release was sustained for almost 56 days.

The T_{max} , C_{max} , and absolute bioavailability values calculated from Fig. 5c are summarized in Fig. 5d. The prolonged release of Dp was observed in all formulations of Dp-PLGA-M, Dp-PLA-M, and Dp-PLA-M/PC. However, the T_{max} , C_{max} , and bioavailability values were significantly different between all formulations. Dp-PLGA-M and Dp-PLA-M exhibited a C_{max} of 6.7 mg/mL at 4 d (T_{max}) and 4.0 mg/mL at 1

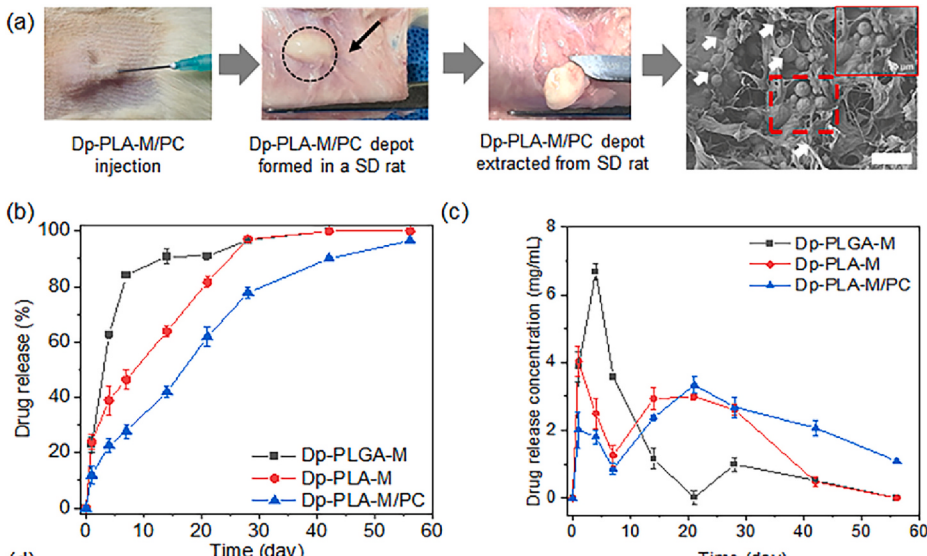


Fig. 5. *In vivo* drug release of Dp-PLGA-M, Dp-PLA-M, and Dp-PLA-M/PC formulations. (a) Images of DP-PLA-M/PC depot formed and removed in an SD rat after injection and SEM images (scale bar: 100 μ m); (b) accumulated *in vivo* release behavior of Dp from Dp-PLGA-M, Dp-PLA-M, and Dp-PLA-M/PC formulations for 56 days; (c) Dp concentration released from each depot at each time point; (d) T_{max} , C_{max} , Dp concentration at C_{max} , and bioavailability (AUC) of the Dp released from each depot of Dp-PLGA-M, Dp-PLA-M, and Dp-PLA-M/PC [^a The data represent the mean \pm SD ($n = 3$); ^b Time of C_{max} ; ^c Dp release amount percent at C_{max} ; ^d Concentration at C_{max} ; ^e AUC value for each formulation for 56 days [^f $p < 0.001$ versus Dp-PLGA-M, Dp-PLA-M, and Dp-PLA-M/PC].

SEM images of Dp-PLGA-M, Dp-PLA-M, and Dp-PLA-M/PC depots formed *in vivo* after subcutaneous injection of each formulation.

Formulation ^a	T_{max} ^b (day)	Release percent at C_{max} ^c (%)	Dp conc. at C_{max} ^d (mg/mL)	AUC_{0-t} ^e (day * mg/mL)
Dp-PLGA-M	4	39.7 \pm 1.4 ^f	6.7 \pm 0.2 ^f	70.9 \pm 2.2 ^g
Dp-PLA-M	1	24.0 \pm 2.6 ^f	4.0 \pm 0.4 ^f	96.6 \pm 5.2 ^g
Dp-PLA-M/PC	21	19.9 \pm 1.3 ^f	3.3 \pm 0.2 ^f	125.8 \pm 3.4 ^g

d (T_{\max}) respectively, and the concentrations decreased rapidly thereafter, approaching 7 $\mu\text{g}/\text{mL}$ at 21 days (for Dp-PLGA-M) and 1.3 mg/mL at 7 days (Dp-PLA-M). Dp-PLA-M/PC showed a 2 mg/mL release rate on day 1, which decreased to nearly 0.9 mg/mL at 7 days. In contrast, Dp-PLA-M/PC showed a C_{\max} of 3.3 mg/mL at 21 days (T_{\max}), then maintained a sustained Dp release profile for 56 days. The T_{\max} and C_{\max} values for Dp-PLA-M/PC were significantly higher and lower, respectively, than those of Dp-PLGA-M and Dp-PLA-M.

The AUC_{0-t} values for Dp-PLGA-M, Dp-PLA-M, and Dp-PLA-M/PC were 70.9, 96.6, and 125.8 mg/mL , respectively. Moreover, the relative bioavailabilities of Dp-PLA-M and Dp-PLA-M/PC were approximately 137% and 188% compared to Dp-PLGA-M.

Collectively, our findings suggested that the differences in the physicochemical properties between the PLGA and PLA carriers or the wrapping of Dp-PLA-M with PC hydrogel increased the bioavailability of the released Dp for the entire release period.

3.7. Morphological changes and biodegradation of *in vivo* formed depot

We next sought to examine the differences in the morphological and biodegradation characteristics of the Dp-PLGA-M, Dp-PLA-M, and Dp-PLA-M/PC depots formed *in vivo*. To achieve this, the *in vivo* formed Dp depots were removed from the SD rats at predetermined times and examined using an optical camera and micro-CT (Fig. 6). The Dp-PLGA-M, Dp-PLA-M, and Dp-PLA-M/PC depots could be easily identified and isolated from the surrounding tissue. The resulting *in vivo* formed Dp depots maintained their shapes even after 6–8 weeks but their sizes decreased gradually after implantation.

First, the width, length, and height of the removed Dp depot were measured with a ruler. The volume of the Dp depot was also calculated via micro-CT. Our findings confirmed that the volume of the Dp depot decreased gradually with implantation time, meaning that the depot was biodegraded.

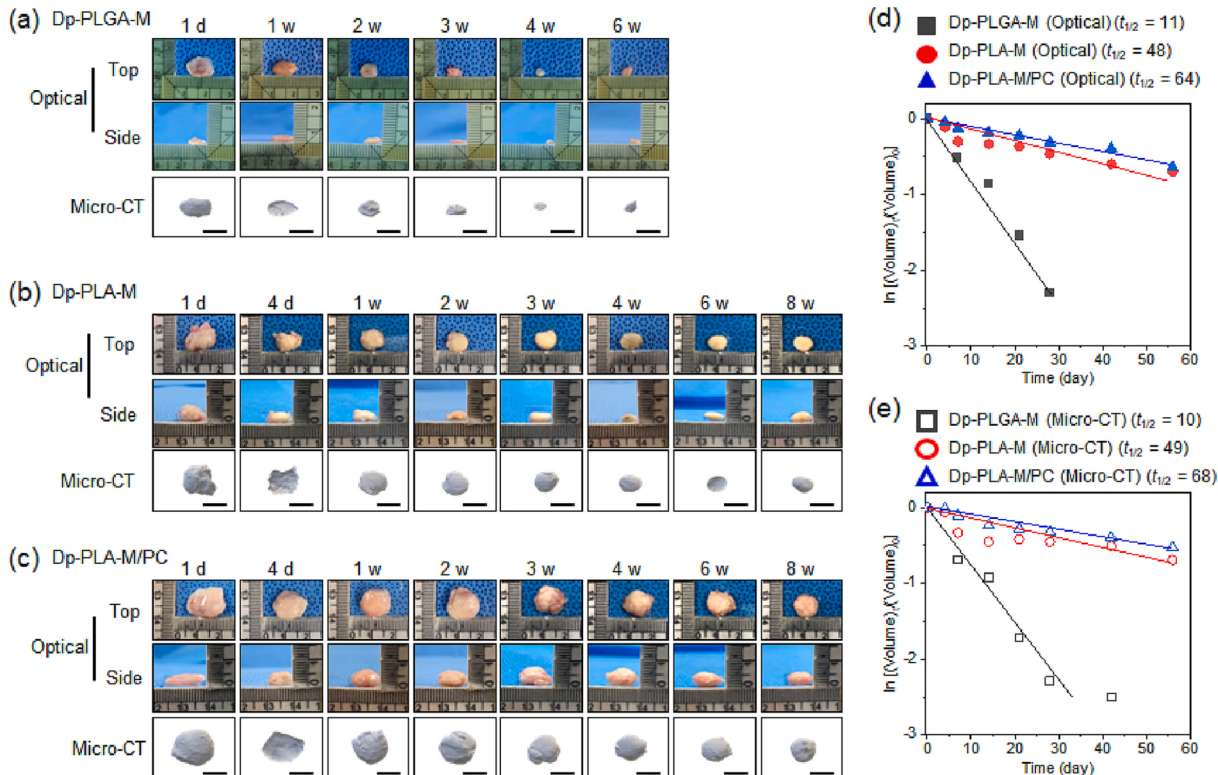


Fig. 6. Volume changes of *in vivo* formed depot. Optical top and side images and micro-CT images of the (a) Dp-PLGA-M, (b) Dp-PLA-M, and (c) Dp-PLA-M/PC depots removed from SD rats at each implantation time (scale bar: 1 mm). (d,e) Log plot of decreasing volume calculated based on (d) optical imaging and (e) micro-CT analyses of the Dp-PLGA-M, Dp-PLA-M, and Dp-PLA-M/PC depots as a function of time.

The Dp-PLGA-M and Dp-PLA-M depots had volumes of approximately 300 and 400 mm^3 (from optical image) and 250 and 300 mm^3 (from micro-CT) on day 1, respectively. After 7 days, the volumes of the Dp-PLGA-M and Dp-PLA-M depots decreased by 50%–56% compared to day 1. Dp-PLGA-M exhibited a volume decrease of 93% at 4 weeks. In contrast, Dp-PLA-M was degraded by approximately 57% at 4 weeks and 66% at 8 weeks. Dp-PLA-M showed a slower decrease in volume compared to Dp-PLGA-M, which was indicative of its slow degradation.

The Dp-PLA-M/PC depot exhibited a large volume of approximately 600 mm^3 (based on optical images) and 560 mm^3 (based on micro-CT analyses) on day 1. The larger size of the Dp-PLA-M/PC depot compared to the Dp-PLA-M depot was likely due to the initial volume of the PC hydrogel. The volume of the Dp-PLA-M/PC depot decreased gradually but it was still 50% of its original size at 8 weeks.

The changes in the volumes of the Dp-PLA-M, Dp-PLGA-M, and Dp-PLA-M/PC depots were plotted as a function of implantation time. The volume change plots determined from optical images and micro-CT analyses were almost identical. The half-life of each depot was calculated from the slope of each plot. The half-lives of the Dp-PLGA-M, Dp-PLA-M, and Dp-PLA-M/PC depots were 10–11, 48–49, and 64–68 days, respectively.

The removed Dp-PLGA-M, Dp-PLA-M, and Dp-PLA-M/PC depots were observed using an optical Camscope and scanning electron microscopy (SEM) (Fig. 7). The Dp-PLGA-M, Dp-PLA-M, and Dp-PLA-M/PC depots in the optical and SEM images were also easily identified and isolated from the surrounding tissue.

The optical Camscope images of the Dp-PLGA-M, Dp-PLA-M, and Dp-PLA-M/PC depots demonstrated that the topical area of the microspheres decreased and the tissue became more organized with implantation time. At four weeks, the microspheres were uniformly covered with tissue, and adherence to the surrounding tissue was more evident. Fragments of the microspheres were interspersed with connective tissue, and there were numerous fibrous tissues beneath the interface area of

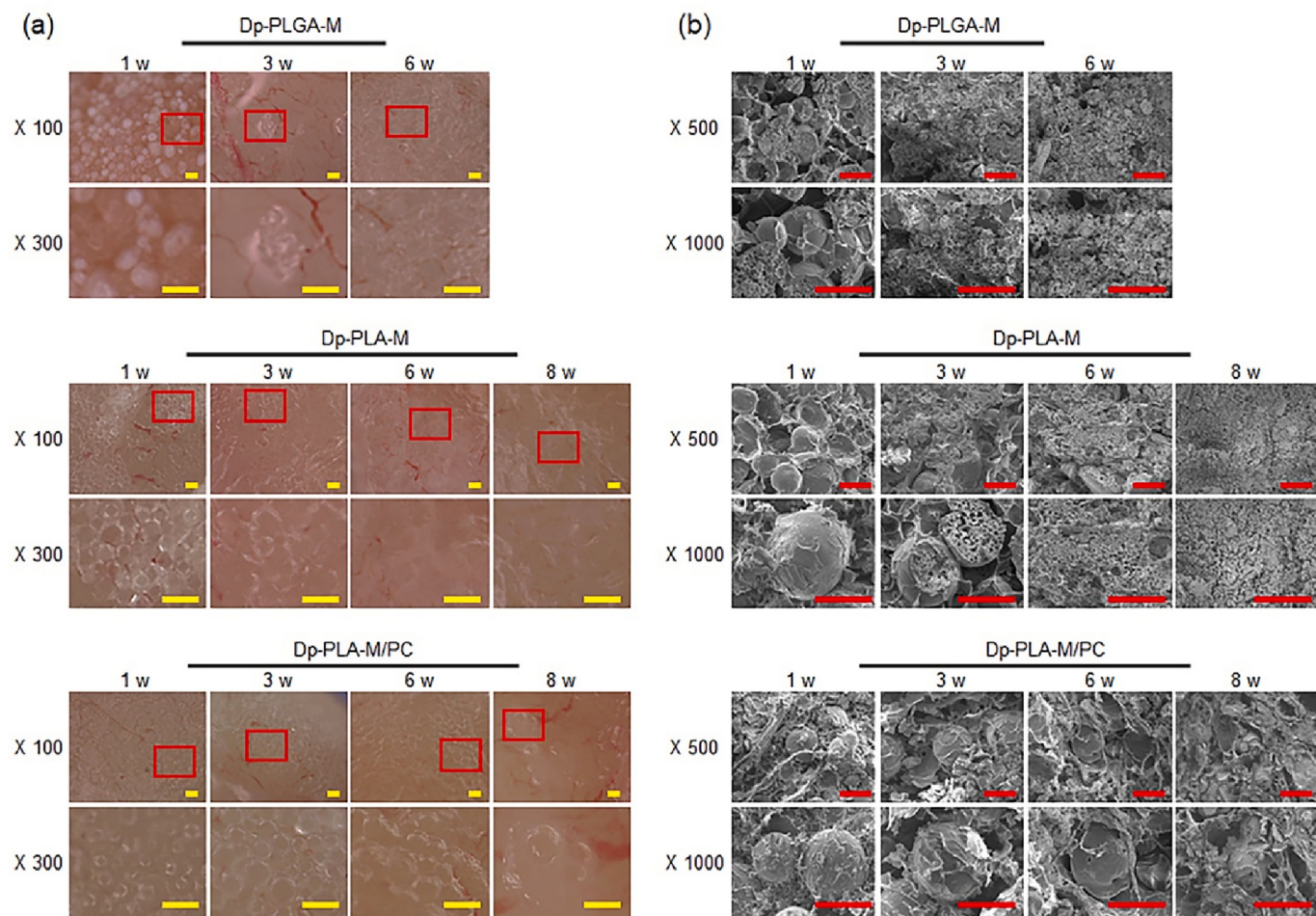


Fig. 7. (a) Optical and (b) SEM images of Dp-PLGA-M, Dp-PLA-M, and Dp-PLA-M/PC depots formed *in vivo* after subcutaneous injection of each formulation (yellow scale bar: 100 μ m, red scale bar: 50 μ m). (For interpretation of the references to color in this figure legend, the reader is referred to the web version of this article.)

the microspheres.

In our SEM analyses, Dp-PLGA-M and Dp-PLA-M spheres and some materials with a distorted shape were observed at one week. At three weeks, there were few spheres in the Dp-PLGA-M depot. Almost no Dp-PLGA-M spheres were observed at six weeks. In contrast, Dp-PLA-M spheres in the *in vivo* formed depot were observed at three weeks and some even at six weeks. Therefore, our observations demonstrated that the Dp-PLA-M spheres remained in the *in vivo* depot for a longer period than Dp-PLGA-M. This was likely due to differences in the *in vivo* biodegradation rates between PLGA and PLA.

Furthermore, Dp-PLA-M/PC exhibited a clear sphere shape for a longer period than Dp-PLA-M. Therefore, we speculated that the PC hydrogel that covered the Dp-PLA-M delayed the biodegradation of the microspheres by *in vivo* biological media and/or enzymes.

The changes in the ^1H NMR spectra of the removed depots of Dp-PLGA-M, Dp-PLA-M and Dp-PLA-M/PC were observed for 8 weeks (Fig. 8a-f). The characteristic lactide (a,c, A,B) and glycolide (b) and spectral peaks of PLGA, PLA, and PCL were observed in the ^1H NMR spectra at week 0 [27,28,33].

The spectrum of PLGA obtained from the Dp-PLGA-M depot exhibited the characteristic peaks of degraded lactide-derived moieties (LAO) and glycolide-derived moieties (GAO), as well as non-degraded PLGA (including oligomers that are difficult to determine) at 1 week. The peaks assignable to the glycolide segment disappeared at 3 weeks. The degraded peak intensities assignable to each moiety increased over time. Finally, no Dp-PLGA-M depot was obtained from animals at 8 weeks, indicating almost complete biodegradation.

Moreover, the spectrum of PLA obtained from the Dp-PLA-M depot exhibited the characteristic peaks of degraded lactide-derived moieties (LAO) and non-degraded PLA at 1 week. PLA-associated peaks persisted at 8 weeks, albeit with markedly lower intensities.

The NMR spectra of Dp-PLA-M/PC showed several peaks assignable to both PLA and PC. The peaks assignable to PC showed almost no changes even after 8 weeks, indicating little to no biodegradation.

However, a slightly degraded peak (A') was observed among the spectral peaks assignable to PLA, which increased slightly as a function of time. However, the A' peak intensities showed minor changes compared with those of Dp-PLA-M. This result indicated that PC delayed the biodegradation of PLA alone even in *in vivo* implantation. Consistent with the findings of our optical, micro-CT, and SEM analyses, the aforementioned results indicated that the PC hydrogel that covered the Dp-PLA-M delayed the biodegradation of the microspheres by *in vivo* biological media and/or enzymes.

Next, the integration of the degraded peak determined from NMR analyses was plotted, and the half-life of the depot was calculated from the slope. The half-lives of the Dp-PLGA-M and Dp-PLA-M depots were 11 and 34 days, respectively.

To assess the *in vivo* degradation of the Dp-PLGA-M, Dp-PLA-M, and Dp-PLA-M/PC depots, the compositions of the depots degraded *in vivo* were monitored via gel permeation chromatography (GPC) (Fig. 8g-j). The results of our GPC analyses showed the changes in the GPC trace from the degraded PLGA and PLA during degradation for 8 weeks *in vivo*. The single peak at low retention times gradually shifted to several low molecular weight peaks at a higher retention time assignable to

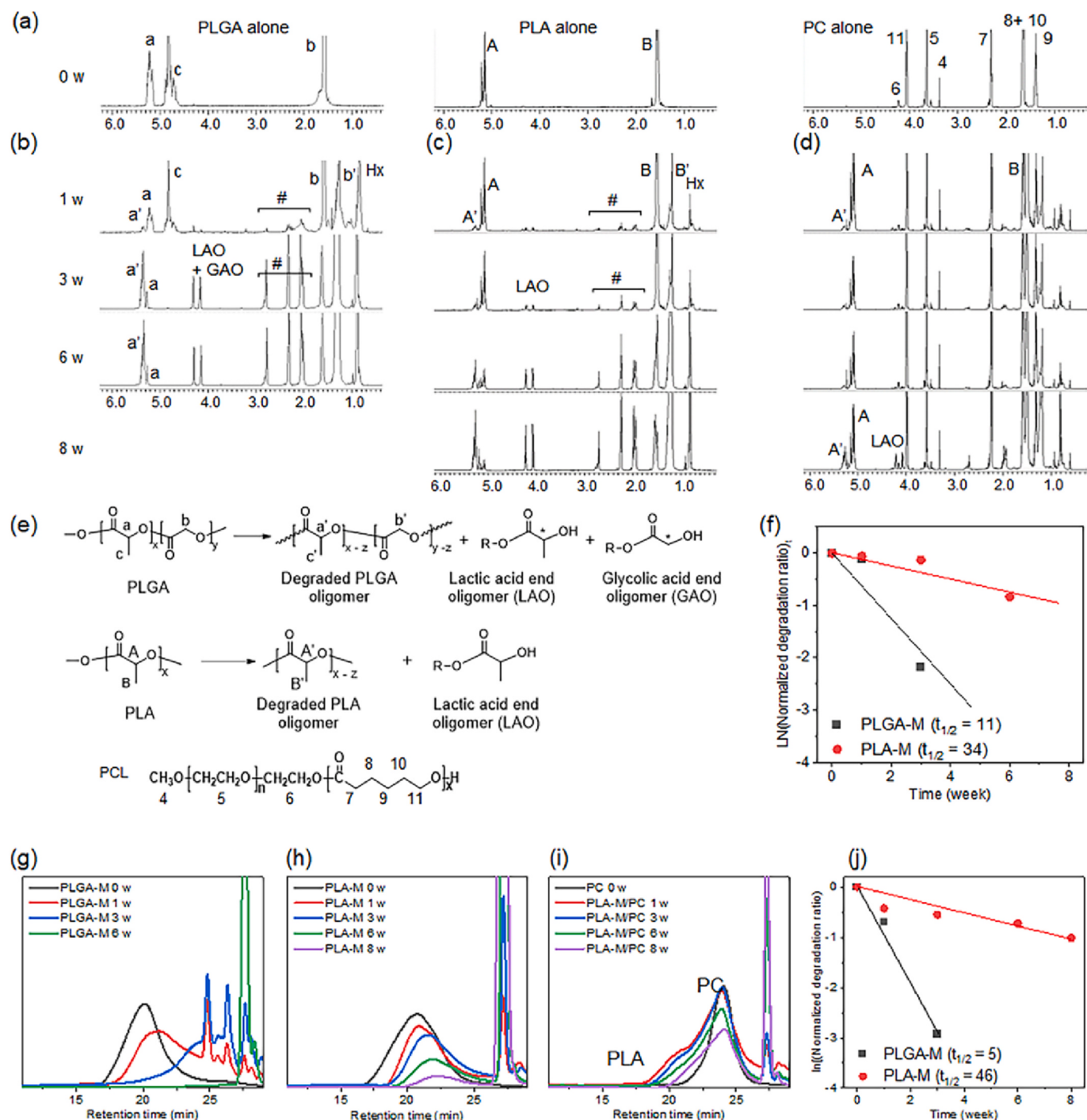


Fig. 8. *In vivo* biodegradation evaluation of Dp-PLGA-M, Dp-PLA-M, and Dp-PLA-M/PC depots formed after *in vivo* subcutaneous injection of injectable formulations: ^1H NMR of (a) original PLGA, PLA, and PC alone. (b) PLGA-M, (d) PLA-M, and (e) PLA-M/PC depots removed from SD rats at 1, 3, 6, and 8 weeks. (e) Plausible degradation products from the biodegradation of PLGA and PLA, and structure of the resulting polycaprolactone (PCL) chain (lactic acid end oligomers [LAO], glycolic acid end oligomers [GAO], degraded PLGA oligomers, and oligomer were difficult to determine [#]). (f) Log plot of integration of degraded peaks (b/b' or B/B') of PLGA or PLA *versus* time, and GPC curve of (g) PLGA-M, (h) PLA-M, and (i) PLA-M/PC depot removed from SD rats at 1, 3, 6, and 8 weeks after *in vivo* subcutaneous injection of injectable formulations. (j) Log plot of PLGA-M and PLA-M degradation.

degradation species, indicating a decrease in molecular weight due to degradation. The peak intensities at low molecular weights corresponded to the degraded oligomers and tended to increase with time.

Dp-PLGA-M and Dp-PLA-M exhibited the characteristic PLGA and PLA peaks and degraded oligomeric species assignable to the degradation of oligomeric PLGA and PLA species as a function of implantation time. Each original PLGA and PLA peak decreased, whereas the degraded oligomeric species increased over time. The PLGA showed

larger degraded oligomeric species than those of PLA, indicating that PLGA had a faster degradation rate. The *in vivo* degradation of Dp-PLGA-M and Dp-PLA-M exhibited a decreasing constant rate with time. These slopes confirmed that Dp-PLGA-M degraded nine times faster than PLA.

GPC analysis of Dp-PLA-M/PC showed bimodal peaks assignable to PLA and PC, and therefore their degradation ratios could not be determined. The intensity of PLA-associated peaks decreased, whereas the PC-associated peaks remained almost unchanged, except for a small low

molecular weight peak corresponding to a degraded PLA species. These results indicated that little degradation occurred even after 8 weeks.

The remaining molecular weights of PLGA and PLA were plotted against the implantation time. The half-life of the Dp-PLGA-M and Dp-PLA-M depots were 5 and 46 days, respectively. The degradation rates of PLGA were shorter than those of PLA.

Collectively, our findings demonstrated that the *in vivo* biodegradation rate of Dp-PLGA-M was approximately 5–9 times faster than that of Dp-PLA-M. This finding was consistent with the generally known phenomenon that the hydrophobicity and crystallinity of PLA suppress the penetration of biological media, thus delaying the biodegradation process. In turn, this delayed biodegradation resulted in a more long-lasting and sustained Dp release from Dp-PLA-M than Dp-PLGA-M.

3.8. *In vivo* histological analysis and biocompatibility evaluation of injectable formulations

Hematoxylin and eosin (H&E)-stained histological sections of harvested Dp-PLGA-M, Dp-PLA-M, and Dp-PLA-M/PC depots demonstrated an increase in the numbers of microspheres interspersed inside connective tissues at the injected. Additionally, there was also an increase in the numbers of macrophages and neutrophils in the border zone and near the microspheres, as well as inside the tissue layer (Fig. 9). Host cells had invaded the Dp-PLGA-M, Dp-PLA-M, and Dp-PLA-M/PC depot, and there was a dense accumulation of inflammatory cells around each microsphere.

At three weeks, the Dp-PLGA-M depot showed a crushed spherical structure, although some of the microspheres were still round. However, it was difficult to find a spherical shape at six weeks, which was likely due to the biodegradation of PLGA. The Dp-PLA-M depot exhibited round microspheres at weeks 1 and 3. However, crushed spherical structures were observed thereafter. Slightly crushed spheres were

observed at six weeks but were difficult to find at eight weeks, indicating the biodegradation of PLA.

In contrast, the Dp-PLA-M/PC microspheres remained spherical for six weeks, albeit with some occasional instances of crushed spheres. Additionally, some spherical or crushed microspheres interspersed inside connective tissue were observed at the injected sites even at eight weeks. Together with the results of the optical, micro-CT, and SEM analyses, the above-described results further suggested that the PC hydrogel wrapped around the PLA microspheres delayed their biodegradation by *in vivo* biological media and/or enzymes.

To assess the local biocompatibility of the Dp-PLGA-M, Dp-PLA-M, and Dp-PLA-M/PC depots, the removed depot tissues were examined by immunohistochemical staining of macrophage marker ED1 antibodies and T lymphocyte marker CD4 to characterize the extent of host cell infiltration and inflammatory response within and near the transplanted microspheres (Fig. 10).

DAPI staining (blue) showed many host cells surrounding the Dp-PLGA-M, Dp-PLA-M, and Dp-PLA-M/PC depots, and ED1 or CD4 staining (pink) showed macrophage or neutrophil accumulation at the surfaces of the Dp-PLGA-M, Dp-PLA-M, and Dp-PLA-M/PC depots and in surrounding tissues after one week.

The numbers of macrophages and neutrophils increased in the border zone and near the microspheres, as well as inside the tissue layer. The tissue adjacent to the microspheres showed a significant number of ED1- and CD4-positive cells. The percentages of ED1- and CD4-positive cells in the Dp-PLGA-M, Dp-PLA-M, and Dp-PLA-M/PC depots after one week were 60% and 42%, 48% and 34%, and 39% and 28%, respectively, indicating that the transplantation of foreign microsphere materials resulted in an acute short-term inflammatory response.

Similarly, the Dp-PLGA-M depots exhibited the highest percentages of ED1- and CD4-positive cells, followed by Dp-PLA-M and Dp-PLA-M/PC. These percentages decreased significantly after 1 week in all

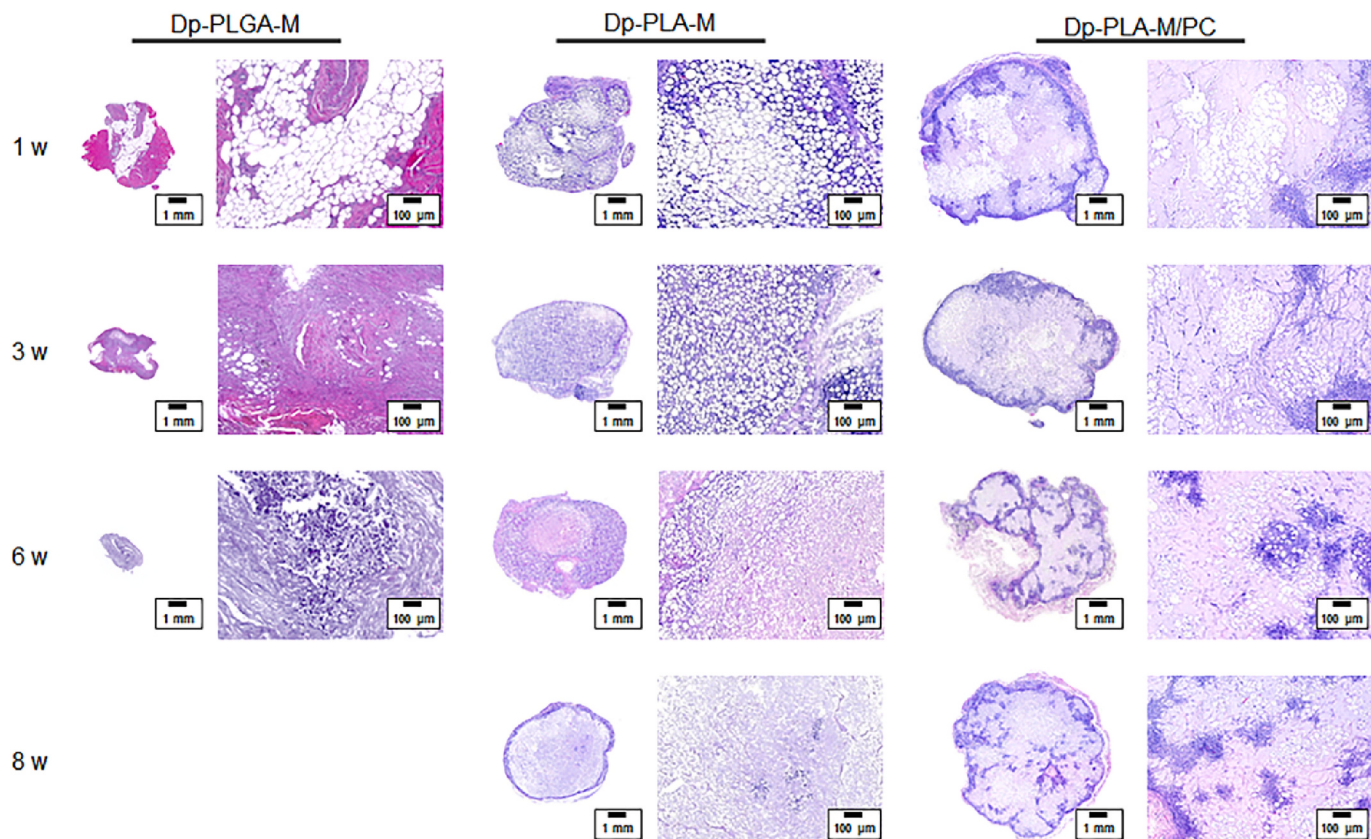


Fig. 9. H&E-stained histological sections of Dp-PLGA-M, Dp-PLA-M, and Dp-PLA-M/PC depots removed from SD rats at 1, 3, 6, and 8 weeks after *in vivo* subcutaneous injection of injectable formulations [full (left) and enlarged (right) images of each of the H&E-stained histological sections are illustrated in the figure].

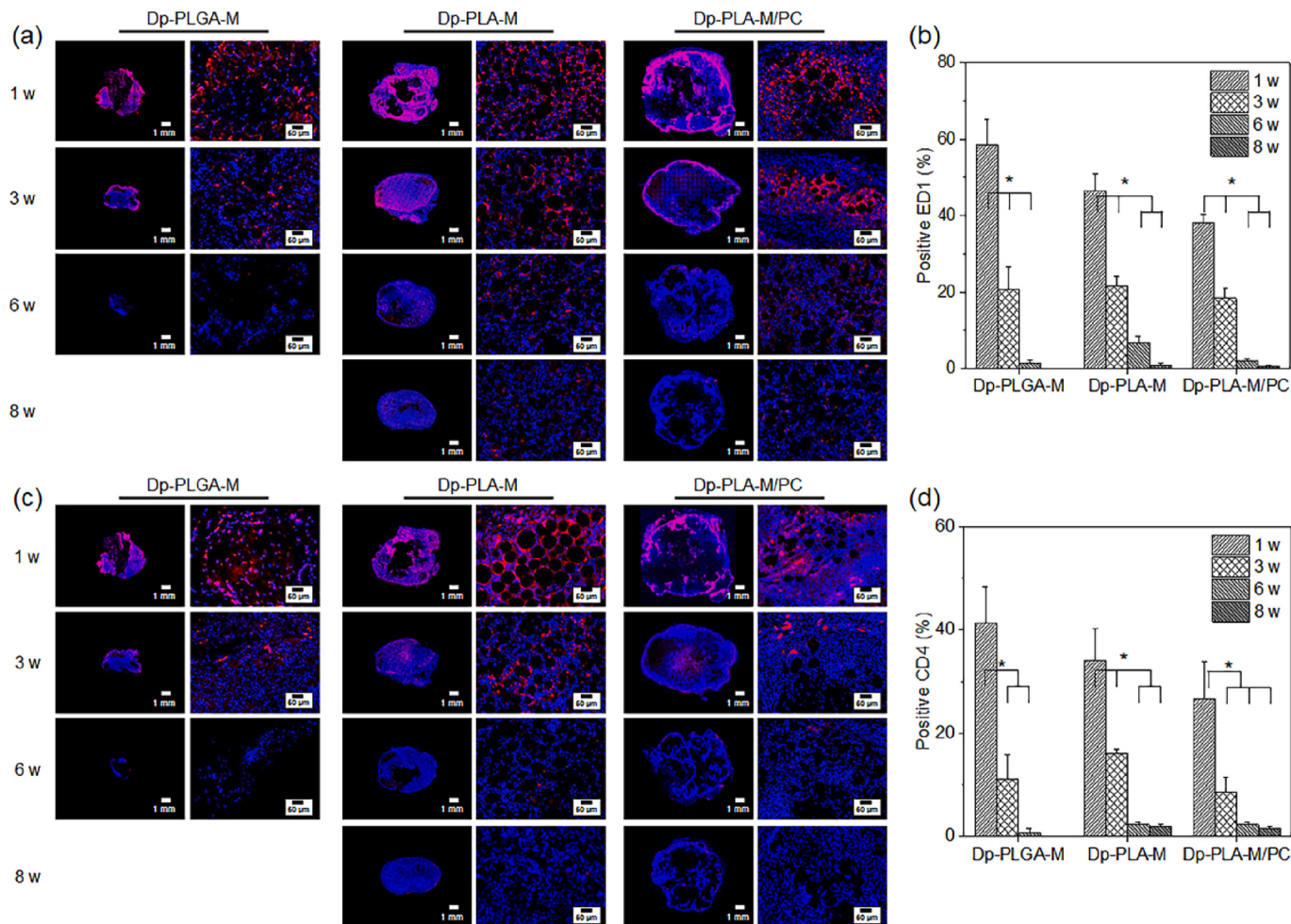


Fig. 10. (a) ED1- and (c) CD4-stained histological sections [full (left) and enlarged (right) images of ED-1 or CD-4 stained histological sections] and the number of (b) ED1- and (d) CD4-positive cells in the Dp-PLGA-M, Dp-PLA-M, and Dp-PLA-M/PC depots removed from SD rats at 1, 3, 6, and 8 weeks after *in vivo* subcutaneous injection of injectable formulations (* $p < 0.01$) [full (left) and enlarged (right) images of each of the ED1- and CD4-stained histological sections are illustrated in the figure].

depots, reaching values that were nearly below 2% at six or eight weeks. This indicated that the rapidly degrading PLGA caused a strong inflammatory response, whereas covering the Dp-PLA-M microspheres with PC hydrogel substantially weakened this inflammatory response.

4. Discussion

Several drug delivery systems have been recently developed to prologue drug release, thus reducing dosing frequency and increasing patient compliance. In previous studies, drug delivery systems have been designed using microspheres, polymeric nanoparticles, micelles, conjugates, vesicles, liposomes, and polyplexes, thus enabling the therapeutic drug to be physically encapsulated, complexed, or chemically conjugated [35–41].

In this study, we chose PLGA and PLA due to their clinical applicability. Specifically, we developed injectable, slow-release formulations of Dp-PLGA-M and Dp-PLA-M to reduce the dosing frequency of Dp even though the PLGA and PLA used in this work have different MW. First, we prepared Dp-PLGA-M and Dp-PLA-M using an ultrasonic atomizer. Dp-PLGA-M and Dp-PLA-M microspheres with a uniform size distribution were repeatedly obtained at a nearly quantitative production yield and with high Dp encapsulation yields.

Higher Dp encapsulation yields are critical to ensure clinical applicability. In this work, the high Dp encapsulation rates obtained using an ultrasonic atomizer could guarantee the repeated and uniform

processing of Dp-PLA-M in mass production. Additionally, fewer microspheres need to be injected due to the higher Dp encapsulation yields. In this work, fewer Dp-PLA-M had to be injected due to the higher Dp loading rates.

The Dp-PLGA-M and Dp-PLA-M microspheres were round and smooth. The prepared Dp-PLGA-M and Dp-PLA-M microspheres had a uniform size with a span value close to 1 and an average particle diameter of 65 μm . Collectively, our findings indicated that Dp-PLGA-M and Dp-PLA-M with a uniform size for animal/clinical injection can be the repeatedly and optimally manufactured using an ultrasonic atomizer.

Additionally, an injectable PC hydrogel was used to wrap the Dp-PLA-M and control the initial release of Dp. In turn, this extended the sustained release period of Dp. We previously reported that PC was an *in situ*-forming hydrogel able to respond to body temperature via hydrophobic interactions [27–30]. The microsphere formulations with PC hydrogels (Dp-PLGA-M/PC, and Dp-PLA-M/PC) exhibited more viscosity and hydrogel-like rheological properties at body temperature than PC alone. These findings suggested that Dp-PLGA-M or Dp-PLA-M with hydrophobic properties can enhance the hydrophobic interaction of PC hydrogels. The Dp-PLGA-M/PC and Dp-PLA-M/PC formulations occurred in solution form when they were below body temperature but became hydrogel depots once they reached body temperature. The formation rate of the depot for Dp-PLGA-M/PC and Dp-PLA-M/PC formulations was observed within 10 s. Therefore, we concluded that

injectable Dp-PLA-M/PC had excellent injectability *in vivo*.

The injectable formulations developed herein exhibited ease of injection, even flow, no clogging, and required little force (*i.e.*, <1 N) to be passed through a 21-G needle. There were slight differences between Dp-PLGA-M and Dp-PLA-M, however, their injectability was largely similar. Nevertheless, some clogging was observed and a strong injection force was required to pass these injectable solutions through needles with small inner diameter gauges of 23-G and 26-G. Therefore, a 21-G needle was deemed the most appropriate for the administration of Dp-PLGA-M and Dp-PLA-M microspheres, which had an average diameter of 65 μm . Microspheres may cause pain during injection and therefore smaller particles may be more desirable, as they allow for the use of thinner syringe needles for injection. In fact, previous studies have confirmed that smaller microspheres cause less pain than larger microspheres because they allow for the use of thinner needles [31,32]. Moreover, microspheres with a diameter of <100 μm were reported to be easily injected using 21–25-G needles [42].

However, if the drug concentrations inside the microspheres are similar, injecting a high density of many small microspheres may also pose a problem. Therefore, microspheres of an appropriate size that can be administered using a 21–25-G needle or thinner needles would undoubtedly make their clinical application more patient-friendly. Therefore, administering the Dp-PLGA-M and Dp-PLA-M with an average diameter of 65 μm prepared herein would likely cause little pain when applied clinically.

The standard manual of the International Organization for Standardization indicates that the injection force for syringes should range between 1 and 4 N in clinical applications [39]. Collectively, our results demonstrated that the Dp-PLGA-M and Dp-PLA-M microspheres could be administered according to clinical guidelines using a 21-G needle.

Generally, PLGA and PLA have several physical and chemical differences, particularly in their crystallinity [18–21,43–46]. In turn, this leads to variations in the physicochemical properties of Dp-PLGA-M and Dp-PLA-M. In this work, we confirmed that Dp-PLA-M had stronger microsphere surface strength and Young's modulus, as well as a higher resistance to deformation than Dp-PLGA-M. This result indicated that the physical properties of Dp-PLGA-M and Dp-PLA-M could be affected by the polymer matrix itself.

During the initial phases of *in vivo* depot formation, the Dp-PLGA-M and Dp-PLA-M microspheres remained spherical, but the spherical shapes were crushed and decreased with implantation time. After 4–6 weeks, Dp-PLGA-M and Dp-PLA-M particles became increasingly difficult to detect.

The first aim of this study was to assess whether the differences between the physicochemical properties of PLGA and PLA had an effect on the sustained Dp release from PLGA and PLA microspheres. In the absence of biological media, Dp-PLA-M were stable at both 4 and 37 °C for 4 weeks, but Dp-PLGA-M showed the stability at only 4 °C for 4 weeks. However, Dp-PLGA-M and Dp-PLA-M aggregated at temperatures above 60 °C even at 1 week. This was likely because PLGA typically shows a glass transition temperature at a 40–60 °C range, whereas PLA ranges from an amorphous glassy polymer to a semi-crystalline and highly crystalline polymer with a glass transition of 60–65 °C and a melting temperature of 130–180 °C.

In current work, Dp-PLGA-M degraded far faster than Dp-PLA-M. Meanwhile, the biodegradation of PLGA and PLA was affected by the penetration of biological media into the depots. Therefore, the delayed biodegradation of PLA compared to PLGA was attributed to its high crystallinity and hydrophobicity. In this work, the *in vivo* biodegradation rate of Dp-PLGA-M and Dp-PLA-M were determined via NMR, micro-CT, and GPC analyses. Due to its crystallinity and hydrophobicity, Dp-PLA-M had a longer biodegradation period than Dp-PLGA-M because it delayed the penetration of biological media.

After comparing the Dp release from Dp-PLGA-M and Dp-PLA-M in this work, we observed a delayed Dp release from Dp-PLA-M. In turn, this resulted in a more sustained and long-lasting Dp release from Dp-

PLA-M than Dp-PLGA-M due to the differences in the biodegradation rates of PLGA and PLA.

Therefore, the PC hydrogel was wrapped with Dp-PLA-M to achieve the second aim of this work. This Dp-PLA-M/PC formulation design focused on the lagging behavior of the Dp released from the surface layer or inside of the Dp-PLA-M. In the present study, we observed a suppression of the initial Dp burst from Dp-PLA-M/PC compared to Dp-PLA-M. It was conjectured that Dp from Dp-PLA-M/PC was diffusely released into the PC hydrogel, after which it was released from the PC hydrogel to the subcutaneous layer during the initial phase. Then, after this initial phase, the Dp released from the Dp-PLA-M passed through the PC hydrogel and then moved to the subcutaneous tissue, resulting in Dp release by lagging behavior. This diffusion delaying process of Dp effectively extended the release time of Dp released from the surface layer or inside Dp-PLA-M. Therefore, we believe that the Dp-PLA-M/PC formulation could achieve a sustained Dp release for longer than two months.

Meanwhile, the biodegradation of PLGA and PLA and the resulting release of foreign materials induced an inflammatory response in the living tissues [47,48]. The fast biodegradation of PLGA triggered a more pronounced increase in macrophages and neutrophils in the injected tissues compared to PLA. Moreover, the inflammatory response induced by the degradation products decreased as implantation time increased, suggesting that the concentration of degradation products also decreased with time.

Furthermore, our findings confirmed that Dp-PLA-M/PC depots were slow to degrade both *in vitro* and *in vivo*. This was likely because wrapping the Dp-PLA-M with PC hydrogel minimized the loss of the Dp-PLA-M matrix through diffusion or contact with biological media or enzymes. Interestingly, the PC hydrogel itself did not fully degrade for the entire duration of our experiments (two months). This is consistent with the fact that PCL is reported to have a half-life of almost two years [49,50]. Therefore, the degradation of the Dp-PLA-M/PC depot was markedly delayed compared with Dp-PLA-M.

Moreover, the PC hydrogel not only delayed the degradation of the microspheres but also allowed for a more sustained and long-lasting Dp release from Dp-PLA-M/PC compared with Dp-PLA-M, in addition to eliciting a weaker inflammatory response.

This study revealed important insights regarding the maintenance of Dp release for longer than one month. Particularly, Dp-PLA-M/PC, a novel formulation, suppressed the initial release of Dp and maintained the Dp release for longer than Dp-PLA-M. Collectively, our findings demonstrated that Dp-PLA-M/PC could effectively reduce dosing frequency for patient compliance.

However, the proposed Dp-PLA-M/PC formulation may have limitations in clinical applications at this stage. Therefore, additional studies are needed to assess the clinical applicability of this Dp-PLA-M/PC formulation.

Nevertheless, it is difficult to predict interspecies differences in clinical applications because pharmacology studies for Dp-PLA-M/PC formulations have only been conducted using small animals. Therefore, future studies must conduct pharmacology studies using large AD animal models. This will provide valuable insight to conduct first-in-human trials using the Dp-PLA-M/PC formulation.

According to the FDA guidelines, the likelihood of approval of a novel material for clinical applications is much higher if its formulation process is easy to implement. Given that the Dp-PLA-M/PC formulation was a combination of Dp-PLA-M and PC hydrogel, the manufacturing of the Dp-PLA-M/PC formulation must be repeatable and reliable. Therefore, additional efforts are needed to ensure the uniformity of Dp-PLA-M and PC hydrogel production, as well as the establishment of quality control guidelines. This would ensure that the Dp-PLA-M/PC formulation possesses the desired physicochemical characteristics, thus enabling the steady release and efficacy of Dp and the clinical applicability of the Dp-PLA-M and PC hydrogel.

In this study, UV light irradiation was utilized for sterilizing the

microspheres. For the clinical utilization of Dp-PLA-M or Dp-PLA-M/PC formulation, an appropriate sterilization strategy (e.g., gamma irradiation, ethylene oxide gas, radiofrequency glow discharge, or UV light) is necessary [51,52]. Previous studies have reported that the drug content inside microspheres, the drug release rate from the microspheres, and the stability of microspheres vary greatly depending on the sterilization method. Therefore, a careful selection of the appropriate sterilization method for Dp-PLA-M or Dp-PLA-M/PC formulations is needed for future clinical applications.

Taken together, our findings demonstrated that the Dp-PLA-M and Dp-PLA-M/PC formulations examined herein could allow for the development of delayed Dp release products in the near future. However, to the best of our knowledge, there are still no FDA guidelines for Dp-PLA-M or Dp-PLA-M/PC formulations, and therefore additional studies are needed to assess the safety and clinical applicability of these materials.

5. Conclusion

We prepared Dp-PLGA-M and Dp-PLA-M with uniform particle sizes using an ultrasonic atomizer. The proposed approach was not only highly repeatable but also delivered high Dp encapsulation yields. Due to its slower degradation rate compared to Dp-PLGA-M, Dp-PLA-M could release Dp more slowly, and wrapping this material with PC hydrogel further slowed down the release of Dp from Dp-PLA-M/PC. Taken together, our findings provide a promising new means for the sustained and long-lasting delivery of Dp *in vivo* and the reduction of dosing frequencies, which could greatly improve the compliance of Alzheimer's disease patients.

Author contributions

Conceptualization, Y.B.J., K.P., and M.S.K.; formal analysis, Y.B.J., S.L., J.H.N., and H.J.J.; data analysis, Y.B.J., S.L., H.J.J., H.E.K., J.H.N., and H.B.L.; methodology, Y.B.J., S.C., and M.S.K.; validation, Y.B.J., S.L., H.J.J., H.E.K., S.C., H.B.L. and M.S.K.; visualization, Y.B.J. and S.L.; funding acquisition, M.S.K.; project administration, K.P. and M.S.K.; supervision, H.B.L. and M.S.K.; writing—original draft, Y.B.J.; writing—review and editing, M.S.K. All authors have read and agreed to the published version of the manuscript.

Declaration of Competing Interest

The authors declare no conflict of interest.

Data availability

No data was used for the research described in the article.

Acknowledgments

This study was supported by the National Research Foundation of Korea (NRF) grants, Creative Materials Discovery Program (2019M3D1A1078938) and Priority Research Centers Program (2019R1A6A1A11051471), and Ministry of SMEs and Startups, TIPS Program (S2846168). The corresponding author appreciate to Ms. Kyoung Suk Ko, Ms. Chanhee Kim and Ms. Sang-Hui Park carried out the repeated manufacturing for large amounts of Dp-PLA-M in MEDIPOL-YMER inc.

Appendix A. Supplementary data

Supplementary data to this article can be found online at <https://doi.org/10.1016/j.jconrel.2023.02.024>.

References

- [1] T. Babic, The cholinergic hypothesis of Alzheimer's disease: a review of progress, *J. Neurol. Neurosurg. Psychiatry* 66 (1999) 137–147.
- [2] B. Wilson, K.M. Geetha, Neurotherapeutic applications of nanomedicine for treating Alzheimer's disease, *J. Control. Release* 325 (2020) 25–37.
- [3] D. Wakhloo, J. Oberhauser, A. Madira, S. Mahajani, From cradle to grave: neurogenesis, neuroregeneration and neurodegeneration in Alzheimer's and Parkinson's diseases, *Neural Regen. Res.* 17 (2022) 2606–2614.
- [4] A. Di Stefano, A. Iannelli, S. Lasserra, P. Sozio, Drug delivery strategies for Alzheimer's disease treatment, *Expert Opin. Drug Del.* 8 (2011) 581–603.
- [5] H. Wang, Y. Zong, Y. Han, J. Zhao, H. Liu, Y. Liu, Compared of efficacy and safety of high-dose donepezil vs standard-dose donepezil among elderly patients with Alzheimer's disease: a systematic review and meta-analysis, *Expert Opin. Drug Saf.* 21 (2022) 407–415.
- [6] Z.Q. Zhao, B.Z. Chen, X.P. Zhang, H. Zheng, X.D. Guo, An update on the routes for the delivery of donepezil, *Mol. Pharm.* 18 (2021) 2482–2494.
- [7] M. Agrawal, S. Saraf, S. Saraf, S.G. Antimisiaris, M.B. Chougule, S.A. Shoyele, A. Alexander, Nose-to-brain drug delivery: an update on clinical challenges and progress towards approval of anti-Alzheimer drugs, *J. Control. Release* 281 (2018) 139–177.
- [8] T. Ramasamy, H.B. Ruttala, B. Gupta, B.K. Poudel, H. Choi, C.S. Yong, J.O. Kim, Smart chemistry based nanosized drug delivery systems for systemic applications: a comprehensive review, *J. Control. Release* 258 (2017) 226–253.
- [9] T. Ramasamy, H.B. Ruttala, S. Munusamy, N. Chakraborty, Jong Oh Kim, Nano drug delivery systems for antisense oligonucleotides (ASO) therapeutics, *J. Control. Release* 352 (2022) 861–878.
- [10] B.S. Kim, J.M. Oh, H. Hyun, K.S. Kim, S.H. Lee, Y.H. Kim, K. Park, H.B. Lee, M. S. Kim, Insulin-loaded microcapsules for *in vivo* delivery, *Mol. Pharm.* 6 (2009) 353–365.
- [11] L. Ruan, M. Su, X. Qin, Q. Ruan, W. Lang, M. Wu, Y. Chen, Q. Lv, Progress in the application of sustained-release drug microspheres in tissue engineering, *Mater. Today Bio.* 16 (2022), 100394.
- [12] J.K. Kim, E.J. Go, K.W. Ko, H.J. Oh, J. Han, D.K. Han, W. Park, PLGA microspheres containing hydrophobically modified magnesium hydroxide particles for acid neutralization-mediated anti-inflammation, *tissue Eng. Regen. Med.* 18 (2021) 613–622.
- [13] K. Park, S. Skidmore, J. Hadar, J. Garner, H. Park, A. Otte, B.K. Soh, G. Yoon, D. Yu, Y. Yun, B.K. Lee, X. Jiang, Y. Wang, Injectable, long-acting PLGA formulations: analyzing PLGA and understanding microparticle formation, *J. Control. Release* 304 (2019) 125–134.
- [14] G.W. Choi, S. Lee, D.W. Kang, J.H. Kim, J.H. Kim, H.Y. Cho, Long-acting injectable donepezil microspheres: formulation development and evaluation, *J. Control. Release* 340 (2021) 72–86.
- [15] D. Kim, T.H. Han, S.C. Hong, S.J. Park, Y.H. Lee, H. Kim, M. Park, J. Lee, PLGA microspheres with alginate-coated large pores for the formulation of an injectable depot of donepezil hydrochloride, *Pharmaceutics* 12 (2020) 311.
- [16] W. Guo, P. Quan, L. Fang, D. Cun, M. Yang, Sustained release donepezil loaded PLGA microspheres for injection: preparation, *in vitro* and *in vivo* study, *Asian, J. Pharm. Sci.* 10 (2015) 405–414.
- [17] P. Zhang, L. Chen, W. Gu, Z. Xu, Y. Gao, Y. Li, In vitro and *in vivo* evaluation of donepezil-sustained release microparticles for the treatment of Alzheimer's disease, *Biomaterials* 28 (2007) 1882–1888.
- [18] G. Reich, Ultrasound-induced degradation of PLA and PLGA during microsphere processing: influence of formulation variables, *Eur. J. Pharm. Biopharm.* 45 (1998) 165–171.
- [19] L.Y. Li, L.Y. Cui, R.C. Zeng, S.Q. Li, X.B. Chen, Y. Zheng, M.B. Kannan, Advances in functionalized polymer coatings on biodegradable magnesium alloys - a review, *Acta Biomater.* 79 (2018) 23–36.
- [20] E. Çatker, M. Güümüşderelioglu, A. Güner, Degradation of PLA, PLGA homo- and copolymers in the presence of serum albumin: a spectroscopic investigation, *Polym. Int.* 49 (2000) 728–734.
- [21] M. Kim, J.H. Kim, S. Kim, R. Maharjan, N.A. Kim, S.H. Jeong, New long-acting injectable microspheres prepared by IVL-DrugFluidic™ system: 1-month and 3-month *in vivo* drug delivery of leuprorelin, *Int. J. Pharm.* 622 (2022), 121875.
- [22] D. Kim, D. Kim, H. Ha, J. Jung, S. Baek, S.H. Baek, T. Kim, J.C. Lee, E. Hwang, D. K. Han, Fat graft with allograft adipose matrix and magnesium hydroxide-incorporated PLGA microspheres for effective soft tissue reconstruction, *tissue Eng. Regen. Med.* 19 (2022) 553–563.
- [23] J.Y. Heo, J.H. Noh, S.H. Park, Y.B. Ji, H.J. Ju, D.Y. Kim, B. Lee, M.S. Kim, An injectable click-crosslinked hydrogel that prolongs dexamethasone release from dexamethasone-loaded microspheres, *Pharmaceutics* 11 (2019) 438.
- [24] D.Y. Kim, D.Y. Kwon, H.W. Seo, J.S. Kwon, B. Lee, D.K. Han, J.H. Kim, B.H. Min, K. Park, M.S. Kim, Injectable *in situ*-forming hydrogels for a suppression of drug burst from drug-loaded microcapsules, *Soft Matter* 8 (2012) 7638–7648.
- [25] D.Y. Kim, D.Y. Kwon, J.S. Kwon, J.H. Park, S.H. Park, H.J. Oh, J.H. Kim, B.H. Min, K. Park, M.S. Kim, Synergistic anti-tumor activity through combinational intratumoral injection of an *in-situ* injectable drug depot, *Biomaterials* 85 (2016) 232–245.
- [26] A.R. Son, D.Y. Kim, S.H. Park, J.Y. Jang, K. Kim, B.J. Kim, X.Y. Yin, J.H. Kim, B. H. Min, D.K. Han, M.S. Kim, Direct chemotherapeutic dual drug delivery through intra-articular injection for synergistic enhancement of rheumatoid arthritis treatment, *Sci. Rep.* 5 (2015) 14713.
- [27] J.I. Kim, D.Y. Kim, D.Y. Kwon, H.J. Kang, J.H. Kim, B.H. Min, M.S. Kim, An injectable biodegradable temperature-responsive gel with an adjustable persistence window, *Biomaterials* 33 (2012) 2823–2834.

- [28] J.S. Kwon, S.M. Yoon, D.Y. Kwon, D.Y. Kim, G.Z. Tai, L.M. Jin, B. Song, B. Lee, J. H. Kim, D.K. Han, B.H. Min, M.S. Kim, Injectable in situ-forming hydrogel for cartilage tissue engineering, *J. Mater. Chem. B* 1 (2013) 3314–3321.
- [29] M.S. Kim, K.S. Seo, G. Khang, C.H. Sun, H.B. Lee, Preparation of methoxy poly(ethylene glycol)/polyester diblock copolymers and examination of the gel-to-sol transition, *J. Polym. Sci. A, Polym. Chem.* 42 (2004) 5784–5793.
- [30] M.S. Kim, H. Hyun, Y.H. Cho, K.S. Seo, W.Y. Jang, S.K. Kim, G. Khang, H.B. Lee, Preparation of methoxy poly(ethyleneglycol)-block-poly(caprolactone) via activated monomer mechanism and examination of micellar characterization, *Polym. Bull.* 55 (2005) 149–156.
- [31] I. Rudnik-Jansen, K. Schrijver, N. Woike, A. Tellegen, S. Versteeg, P. Emans, G. Mihov, J. Thies, N. Eijkelpamp, M. Tryfonidou, L. Creemers, Intra-articular injection of triamcinolone acetonide releasing biomaterial microspheres inhibits pain and inflammation in an acute arthritis model, *Drug Deliv.* 26 (2019) 226–236.
- [32] J.H. Kim, C.H. Ryu, C.H. Chon, S. Kim, S. Lee, R. Maharjan, N.A. Kim, S.H. Jeong, Three months extended-release microspheres prepared by multi-microchannel microfluidics in beagle dog models, *Int. J. Pharm.* 608 (2021), 121039.
- [33] A. Butreddy, R.P. Gaddam, N. Kommineni, N. Dudhipala, C. Voshavar, PLGA/PLA-based long-acting injectable depot microspheres in clinical use: production and characterization overview for protein/peptide delivery, *Int. J. Mol. Sci.* 22 (2021) 8884.
- [34] H. Hyun, M.S. Kim, S.C. Jeong, Y.H. Kim, S.Y. Lee, G. Khang, H.B. Lee, Preparation of diblock copolymers consisting of methoxy poly(ethylene glycol) and poly(ϵ -caprolactone)/poly(L-lactide) and their degradation property, *Polym. Eng. Sci.* 46 (2006) 1242–1249.
- [35] M. Ye, S. Kim, K. Park, Issues in long-term protein delivery using biodegradable microparticles, *J. Control. Release* 146 (2010) 241–260.
- [36] S.P. Schwendeman, R.B. Shah, B.A. Bailey, A.S. Schwendeman, Injectable controlled release depots for large molecules, *J. Control. Release* 190 (2014) 240–253.
- [37] T. Ramasamy, S. Munusamy, H.B. Ruttala, J.O. Kim, Smart nanocarriers for the delivery of nucleic acid-based therapeutics: a comprehensive review, *Biotechnol. J.* 16 (2021), 1900408.
- [38] S. Kim, M. Shin, Role of free catecholamine in thiol-ene crosslinking for hyaluronic acid hydrogels with high loading efficiency of anticancer drugs, *Tissue Eng., Regen. Med.* 19 (2022) 281–287.
- [39] C. Zhang, L. Yang, F. Wan, H. Bera, D. Cun, J. Rantanen, M. Yang, Quality by design thinking in the development of long-acting injectable PLGA/PLA-based microspheres for peptide and protein drug delivery, *Int. J. Pharm.* 585 (2020), 119441.
- [40] H. Hyun, Y.H. Kim, I.B. Song, J.W. Lee, M.S. Kim, G. Khang, K. Park, H.B. Lee, In vitro and in vivo release of albumin using biodegradable MPEG-PCL diblock copolymer as an in situ gel forming carrier, *Biomacromolecules* 8 (2007) 1093–1100.
- [41] S. LaRue, J. Malloy, Evaluation of the dual-chamber pen design for the injection of exenatide once weekly for the treatment of type 2 diabetes, *J. Diabetes Sci. Technol.* 9 (2015) 815–821.
- [42] J.M. Ramstack, G.I. Riley, S.E. Zale, J.M. Hotz, O.F.L. Johnson, Preparation of injectable suspensions having improved injectability, 2003, US6667061.
- [43] P. Lu, G. Wang, T. Qian, X. Cai, P. Zhang, M. Li, Y. Shen, C. Xue, H. Wang, The balanced microenvironment regulated by the degradants of appropriate PLGA scaffolds and chitosan conduit promotes peripheral nerve regeneration, *Mater. Today Bio.* 12 (2021), 100158.
- [44] J.H. Park, B.K. Lee, S.H. Park, M.G. Kim, J.W. Lee, H.Y. Lee, H.B. Lee, J.H. Kim, M. S. Kim, Preparation of biodegradable and elastic poly(ϵ -caprolactone-co-lactide) copolymers and evaluation as a localized and sustained drug delivery carrier, *Int. J. Mol. Sci.* 18 (2017) 671.
- [45] J.H. Park, H.J. Kang, D.Y. Kwon, B.K. Lee, B. Lee, J.W. Jang, H.J. Chun, J.H. Kim, M.S. Kim, Biodegradable poly(lactide-co-glycolide-co- ϵ -caprolactone) block copolymers - evaluation as drug carriers for a localized and sustained delivery system, *J. Mater. Chem. B* 3 (2015) 8143–8153.
- [46] P. Zamiri, Y. Kuang, U. Sharma, T.F. Ng, R.H. Busold, A.P. Rago, L.A. Core, M. Palasis, The biocompatibility of rapidly degrading polymeric stents in porcine carotid arteries, *Biomaterials* 31 (2010) 7847–7855.
- [47] M.S. Kim, H.H. Ahn, M.H. Cho, Y.N. Shin, G. Khang, H.B. Lee, An in vivo study of the host tissue response to subcutaneous implantation of PLGA- and/or porcine small intestinal submucosa based scaffolds, *Biomaterials* 28 (2007) 5137–5143.
- [48] B.S. Kim, J.M. Oh, K.S. Seo, J.S. Cho, K.S. Kim, B. Lee, G. Khang, H.B. Lee, K. Park, M.S. Kim, BSA-FITC loaded microcapsules for in vivo delivery, *Biomaterials* 30 (2009) 902–909.
- [49] H. Sun, L. Mei, C. Song, X. Cui, P. Wang, The in vivo degradation, absorption and excretion of PCL-based implant, *Biomaterials* 27 (2006) 1735–1740.
- [50] S.H. Park, J.S. Kwon, B.S. Lee, J.H. Park, B.K. Lee, J. Yun, B.Y. Lee, J.H. Kim, B. H. Min, T.H. Yoo, M.S. Kim, BMP2-immobilized injectable hydrogel for osteogenic differentiation of human periodontal ligament stem cells, *Sci. Rep.* 7 (2017) 6603.
- [51] N. Umeki, T. Sato, M. Harada, J. Takeda, S. Saito, Y. Iwao, S. Itai, Preparation and evaluation of biodegradable microspheres containing a new potent osteogenic compound and new synthetic polymers for sustained release, *Int. J. Pharm.* 392 (2010) 42–50.
- [52] Y.S. Tapia-Guerrero, M.L. Del Prado-Audelo, F.V. Borbolla-Jiménez, D.M. G. Gomez, I. García-Aguirre, C.A. Colín-Castro, J.A. Morales-González, G. Leyva-Gómez, J.J. Magaña, Effect of UV and gamma irradiation sterilization processes in the properties of different polymeric nanoparticles for biomedical applications, *Materials (Basel)* 13 (2020) 1090.